Aus dem Institut für Biosynthese neuraler Strukturen des Zentrums für Molekulare Neurobiologie Hamburg des Universitätsklinikum Hamburg-Eppendorf
Direktorin: Frau Prof. Dr. Melitta Schachner

Impacts of conditional ablation of the cell adhesion molecule CHL1, the close homologue of L1, on forebrain regions of the mouse

Dissertation

zur Erlangung des Grades eines Doktors der Medizin
dem
Fachbereich Medizin der Universität Hamburg vorgelegt
von

Lena Horn

Hamburg 2009

Angenommen von der Medizinischen Fakultät

der Universität Hamburg am:

Veröffentlicht mit der Genehmigung der Medizinischen

Fakultät der Universität Hamburg

Prüfungsausschuss, der/die Vorsitzende: Prof. Dr. Melitta Schachner

Prüfungsausschuss: 1. Gutachter/in: Prof. Dr. Andrey Irintchev

Prüfungsausschuss: 2. Gutachter/in: Prof. Dr. Michail Davidoff

CONTENTS

1 Introduction

1.1 Cell adhesion and neurodevelopment

Thiery (2003) postulated that cell division, migration and differentiation as well as apoptosis are processes tightly linked in a complex web of signaling pathways essential for all aspects of development. The unique brain architecture is based on adhesive contacts. These contacts contain cell-to-cell and cell-to-matrix connection, allowing interactions between cells themselves and their environment. Cells and axon growth cones migrate toward precise targets guided by specific local and distant cues. This connectivity is necessary for building the brain and for its later function (Goodman and Shatz, 1993; Reichert and Boyan, 1997; Schachner, 1997). To achieve its adult topography and mature function, the brain fine-tunes itself by overproduction, suggested to maximize the information carrying capacity of the immature brain. With the onset of puberty elimination of cells, synapses and receptors seem to rationalize synaptic efficiency in a regionally specific manner (Andersen, 2003; Feinberg, 1982; Walker, 1994). The neuronal network formation depends of contact building, which is influenced by a multitude of membrane-associated cell adhesion molecules (CAMs). The immunoglobulin-like gene superfamily seems to play a leading role in CAMs influence in brain formation and later in brain functioning (Brummendorf and Rathjen 1995). These CAMs can be categorized into different subfamilies on the basis of their overall domain arrangement, membrane topology, and sequence similarity.

1.2 Adhesion molecules

Adhesions molecules are subdivided into three groups: 1/ Cell adhesion molecules (CAMs), including the L1 family of proteins (see below), 2/ Substrate adhesion molecules (SAMs), which are proteins of the extracellular matrix, like collagen or proteoglycanes, and 3/ Cell-joining molecules (CJMs), building strong intercellular connections via desmosomes or gap junctions. In contrast to the CJMs, cell adhesion molecules enable rather loose connections between cells which allow recognition and responses to cues in the cell environment. Individual CAMs can interact with themselves or with other types of molecules, interactions designated respectively as homophilic and heterophilic. CAMs are expressed at the cell surface and can be

classified into four groups: selectins, catherins, intergrins and members of the immunoglobulin (Ig) superfamily.

1.3 Ig superfamily

The three subgroups of the Ig superfamily are defined by the number of Ig-like domains, number of fibronectin repeats and the mode of attachment to the cell membrane (Cunningham, 1995). The molecules belonging to subgroup 1 of the Ig superfamily contain only Ig-like domains, these in subgroup 2 contain Ig-like domains and FN domains and the proteins in subgroup 3 contains Ig-like domains and different other domains. The CAM close homologue of L1 (CHL1), which is in the focus of this study, belongs, together with other well-characterized CAMs like the neural cell adhesion molecule (NCAM) and L1, to subgroup 2 of the Ig superfamily and contains both Ig-like domains and fibronectin type 3 repeats. The common ancestry of the immunoglobulins and the cell adhesion molecules is reflected in the Ig-like domains of both of them. These domains play an important role in recognition events (Edelmann, 1970).

There are characteristic temporal, spatial and cell type-specific expression patterns of the different members of the Ig superfamily neural recognition molecules. Different cell-adhesion molecules are bonded at different stages of development in processes as diverse as cell positioning, tissue pattering and compartmentalization, axon guidance and synaptogenesis (Thiery, 2003).

1.3.1 The L1 family of CAMs

The L1 family of neural recognition molecules is a subgroup of the Ig superfamily (Brümmendorf and Rathjen, 1993). L1 family members have been found in different species, from invertebrates to mammals. In vertebrates, the L1 family consists of four members: L1, CHL1, neurofascin and Nr-CAM (Bixby et al., 1988; Collinson et al., 1998; Holm et al., 1996). They have similar structure consisting of six extracellular C2-type Ig-like domains, four to five fibronectin type 3 repeats, a single transmembrane stretch and a highly conserved cytoplasmic domain that binds the actin cytoskeletal adapter ankyrin. The CAMs of the L1 family are involved in neurite growth and fasciculation, cell adhesion and survival, axon guidance, synaptogenesis and synaptic plasticity (Panicker et al., 2003; Pratte et al., 2003), events underlying normal development of neuronal circuitries and cognitive functions (Wei et al., 1998). These

molecules are expressed in overlapping, but also distinct, patterns at different developmental stages. Their expression continues in some areas in the adult nervous system typically characterized by high levels of synaptic plasticity. The complexity of interactions involving the L1 family members is further influenced by distinct biochemical modifications that include O-glycosylation, amidation, myristoylation, and phosphorylation of specific highly conserved tyrosin and serine residues.

1.3.1.1 **L1**

L1 is a transmembrane glycoprotein of approximately 200 kDa with six 6 immunoglobulin type C2-like domains followed by five fibronectin type 3 domains, a single transmembrane region of 23 hydrophobic residues and a cytoplasmic domain (Moos et al., 1988; Schachner, 1991). In humans, the core protein consists of 1256 amino acids. L1 is highly conserved among mammals, with 80-95% amino acid homology for the extracellular domains, and complete homology of the cytoplasmic domain (Hlavin and Lemmon, 1991). The L1 gene is located on the X chromosome in both humans and mice. It is composed of 28 exons, two of which are alternatively spliced. These two exons, exon 2 and exon 27, are expressed in neurons but not in other L1-expressing cells such as Schwann cells, melanocytes or lymphocytes (Takeda et al., 1996). Exons 3-14 encode the immunoglobulin domains, exons 15-24 - the five fibronectin domains, exon 25 - the transmembrane domain and exons 26-28 - the cytoplastic domain. During CNS development, L1 is expressed on the surface of axons and growth cones and in migrating neurons and, thus, influences axon guidance and cell migration. It continues to be expressed in the adult on the surface of unmyelinated axons. L1 purified from brain or expressed in fibroblasts serves as an excellent substrate for neurite outgrowth (Lagenaur and Lemmon, 1987). It binds homophilically to L1 (Zhao and Siu, 1995) and binds heterophilically to several Ig superfamily adhesion molecules: axonin-1/TAG-1 (Rader et al., 1996), F3/F11/contactin (Brümmendorf T, Rathjen FG, 1993) and DM1-GRASP (DeBernado and Chang, 1996). A cis association of axonin-1 and L1 in the plane of the axonal membrane plays a crucial role in L1-mediated neurite growth (Stoeckli et al., 1996). Homophilic and heterophilic binding of L1 between cells activates intracellular signal transduction cascades involving tyrosine kinases and phosphatases that are essential for neurite outgrowth *in vitro* (Atashi et al, 1992; Ignelzi et al., 1994; Klinz et al., 1995; Saffell et al., 1997). Antibodies to L1 influence intracellular second messengers such as inositol phosphates, Ca^{2+} and pH in

neural cells (Schuch et al., 1989). Ablation of L1 expression in neurons eliminates neurite growth stimulated by L1 offered as a substrate. This is consistent with the idea that L1-mediated neurite growth occurs via a homophilic binding mechanism with substrate-bound L1 (Kenwrick et al, 2000; Lemmon et al, 1989; Fransen et al., 1998). L1 is involved in the outgrowth, pathfinding and fasciculation of axons, in growth cone morphology, neural migration, neuron-neuron adhesion, and neuron-Schwann cell adhesion. L1 may also have a role in learning and memory, because antibodies to L1 perturb the induction of long-term potentiation in rat hippocampal slices (Lüthl et al., 1994) and prevent passive avoidance learning in the chick (Scholey et al., 1993). In addition, L1 contributes to the regeneration of damaged nerve tissue (Lu et al., 2007; Mason et al., 2003; Chaisuksunt et al., 2000).

1.3.1.2 **CHL1**

CHL1 has an amino acid sequence which is ~ 60 % identical to L1 in the extracellular region and ~ 40 % in the cytoplasmic domain (Holm et al., 1996). CHL1 has an N-terminal signal sequence, six immunglobulin like domains, 4.5 fibronectin type 3-like repeats, a transmembrane domain, an intracellular domain of ~ 100 amino acids and a C-terminal. CHL1 has two major isoforms of apparent molecule masses of 185 (substrate-bound) and 165 kDa (soluble form), and a minor isoform of 125 kDa (soluble form) at all stages of brain development (Hillenbrand et al., 1999). CHL1 is glycosilated and about 15% of the total molecular mass of the two major CHL1 isoforms is attributed to N-linked glycans.

Aggregation assays with CHL1-transfected cells have shown that CHL1 is involved neither in homophilic CHL1-CHL1 interactions nor in heterophilic adhesion with L1 (Hillenbrand et al., 1999). CHL1 is first expressed at times of neurite outgrowth during brain development, and is detectable in subpopulations of neurons, astrocytes, oligodendrocyte precursors and Schwann cells of the mouse and rat (Hillenbrand et al., 1999). *In vivo*, the expression of CHL1 by astrocytes appears to be restricted to subpopulations of cells, e.g. astrocytes in the lamina cribosa of the optic nerve (Holm et al., 1996). In the peripheral nervous system, immature and non-myelinating Schwann cells express CHL1 *in vivo*. Oligodendrocyte progenitor cells express CHL1 *in vitro* and downregulate CHL1 expression as they differentiate. Mature oligodendrocytes do not express CHL1 RNA *in vivo* (Holm et al., 1996).

CHL1 show high expression levels in brain regions such as the cerebral cortex, the thalamus, the hippocampus and the amygdala. It is expressed in cerebellar granule cells only after migration in the inner granule layer. In mice, CHL1 is first detectable in the brain at embryonic day 13. Its expression reaches highest levels between embryonic day 18 and postnatal day 7 and declines there after as the brain matures (Hillenbrand et al., 1999).

CHL1 is a strong promoter of neurite outgrowth *in vitro* (Hillenbrand et al., 1999) and promotes neuronal survival. It can prevent death of cerebellar granule neurons and hippocampal neurons *in vitro* (Chen et al., 1999), and promotes neurite outgrowth by hippocampal and small cerebellar neurons in substrate-bound and soluble form (Hillenbrand et al., 1999). CHL1 has the potential to promote embryonic cortical neuron migration through ß1 integrin (Demyanenko et al., 2004), and to promote radial migration by modulation of cytoskeletal dynamics and cell adhesion through ankyrin binding (Buhusi et al., 2003). CHL1 is an enhancer of integrin-mediated cell migration that may be physiologically important in regulating cell migration during cortical development (Buhusi et al., 2003).

During development, CHL1 is expressed at highest levels in the caudal cerebral cortex and at low level in the rostral cortex (Liu et al., 2000) during the period of neuronal progenitor migration from ventricular zone to the cortical plate (Angevine and Sidman, 1961). CHL1 mRNA is localized in a spatially and temporally graded pattern in migrating neuronal precursors and in differentiating, postmitotic pyramidal neurons enriched in layer V (Hillenbrand et al., 1999; Lui et al., 2000). The staining of CHL1 is most prominent in the intermediate zone, which contains radially and tangentially migrating precursors. By postnatal day 0, strongest staining in the mouse-brain is observed in the visual cortex. Staining in the motor cortex is mostly restricted to layer 1. In 7-day-old mice, CHL1 RNA expression is strongest in pyramidal cells of hippocampus, especially the CA1 region, while CHL1 RNA is not detectable in granule cells of the dentate gyrus. Interneurons of the hippocampus proper also express CHL1 RNA. In contrast, in 3-week old mice CHL1 RNA is prominent in granule cells of the dentate gyrus, but is down-regulated in the cerebral cortex. Thalamic neurons do not express CHL1 any more in 3-week-old mice. Expression by cells of subthalamic nuclei and the nucleus lateralis habenulae remains high. Small cerebellar neurons derived from 6 to 7 day-old-mice did not express CHL1, but expressed high levels of L1. Primary cultures of the mesencephalon of embryonic rats also expressed CHL1.

1.4 CAM mutations in human and mice

A large number of molecules are assumed to be involved in cell adhesion and many of these adhesion molecules likely share similar functions. A conservative estimate suggests that 4 – 5% of the human genome is dedicated to adhesion molecules including 865 members of the Ig superfamily (Thiery, 2003). Generation and analyses of mice deficient in such molecules has often suggested that many gene products are dispensable for normal brain development and function due to redundancy (Thiery, 2003). However, humans and mice with mutations in the L1 or CHL1 genes have specific phenotypes indicating unique roles of these molecules in brain development.

1.4.1 L1 mutations

In humans, mutations in the L1 gene, located at Xq28 (Schrander-Stumpel et al., 1992), lead to a wide range of clinical disorders now referred to as L1 disease which includes syndromes like X-linked hydrocephalus due to stenosis of the aqueduct of Sylvius (HSAS), spastic paraplegia type-1, X-linked agenesis of the corpus callosum and MASA syndrome (mental retardation, aphasia, shuffling gait, adducted thumbs). The main symptoms include corpus callosum hypoplasia, mental retardation, adducted thumbs, spastic paraparesis and hydrocephalus. Mental retardation is the most common symptom among individuals with L1 mutations, including patients without hydrocephalus. The mental retardation is often profound, resulting in IQs below 50. L1-associated mental retardation is probably due to abnormal CNS development rather than a result of hydrocephalus (Kamiguchi et al., 1997). A sign of abnormal development is the absence or hypotrophy of the pyramids in patients with L1 disease (Yamasaki et al., 1995). The abnormal development of the corticospinal tract may contribute to the gait disturbances or paraplegia present in many patients. Other developmental abnormalities include hypoplasia of the anterior vermis of the cerebellum, abnormalities in corpus callosum, and thalamus, all pointing to a defect associated with the midline development due to abnormal cell migration (Kamiguchi et al., 1997; Kaplan, 1983). More than 75 different L1 mutations have been reported in the literature. These mutations can be classified into three categories (Van Camp et al., 1996). In the first group, the mutations affect the cytoplasmic domain of L1 as a result of missense or nonsense mutation, frameshifts, duplications or deletions. The second class includes missense point mutations in the extracellular domain. This type of mutations may impair both L1 homophilic and heterophilic binding (Zhao and Siu, 1996). It might also

disrupt the cis interactions that are important in L1-mediated neurite growth and might prevent a change in the conformation of L1 that is required for the production of intracellular signals initiated by L1 binding (Kamiguchi et al., 1997). Class three mutations include those that result in a premature stop codon in the extracellular domain. It might lead to weaker homophilic and heterophilic bindings and also impairments of signal transduction events mediated by the L1 cytoplasmic domain (Kamiguchi et al., 1997). Enlargement of the ventricles is associated with all three classes of mutations. The increase in ventricle volume results from loss of white and gray matter. The loss of L1-mediated adhesion in class 2 and 3 mutations is responsible for severe hydrocephalus. Abnormalities such as fused thalami, flat quadrageminal plates, and failure of cells to reach target zones such as the anterior vermis and neocortex have been linked to loss of L1-mediated adhesion and subsequent abnormal migration of immature neurons from proliferative zones (Kamiguchi et al., 1997). Polymorphisms in L1 genes have been linked to increased risk for schizophrenia (Kurumaji et al., 2001; Sakurai et al., 2002).

L1-null mutant mice display features of the L1 disease including axon guidance errors in the corticospinal tract and corpus callosum, enlarged ventricles, dendrite abnormalities of cortical pyramidal neurons, reduced number of hippocampal neurons, mislocation of dopaminergic neurons and defects in spatial memory (Pratte et al., 2003; Cohen et al., 1997; Dahme et al., 1997).

1.4.2 **CHL1 mutations**

The importance of CHL1 for nervous system development has been shown for the first time in mice deficient in the expression of CHL1 (Montag-Sallaz et al., 2002). CHL1 deficient mice have aberrant projections of hippocampal mossy fibers and of olfactory axons. The behavior of CHL1 deficient mice in the open field, the elevated plus maze, and the Morris water maze test indicate that the mutant mice react differently to their environment than wild-type control littermates. Interestingly, expression of mRNA of the synapse-specific isoform of the neural cell adhesion molecule N-CAM, N-CAM180, is up-regulated in CHL1 deficient mice, whereas mRNA levels of several other recognition molecules are not changed. These observations show that the complete absence of CHL1 during development results in aberrant connectivity and altered exploratory behavior in a novel environment. Another study (Demyanenko et al., 2004) has shown that CHL1 is important for normal cortical

development. In CHL1 deficient mice, the pyramidal neurons in layer V of the visual cortex are deeply displaced and have inverted polarity, while neurons in the somatosensory cortex have improperly oriented apical dendrites, features that are in agreement with a rostro-caudal gradient of CHL1 expression during embryonic development (Liu et al., 2000). While cognitive, motor and olfactory functions in adult CHL1-/- mice are normal, their reactivity to environmental stimuli, social interactions and ability to gate the flow of sensorimotor information are reduced (Irintchev et al., 2004; Morellini et al., 2007). CHL1 is essential for inhibitory synaptic transmission during early postnatal life in mice (Nikonenko et al., 2006). Increased numbers of interneurons and perisomatic inhibitory input to CA1 pyramidal neurons were found in juvenile (3- to 4-week-old) CHL1-/- mice, in association with reduced LTP at CA3-CA1 excitatory synapses. Synaptic abnormalities in CHL1 deficient mice may be related to impairment of synaptic vesicle recycling, a process regulated by CHL1 (Leshchyns'ka et al., 2006).

1.4.2.1 **CHL1 and schizophrenia**

Polymorphisms in the CHL1 gene have been linked to an increased risk to develop schizophrenia (Kurumaji et al., 2001; Sakurai et al., 2002). Sakurai et al. (2002) have identified a missense polymorphism (Leu17Phe) in the CHL1 gene in a Japanese population sample and examined the association between the Leu17Phe polymorphism and schizophrenia. The frequency of leucin at amino acid position 17 has been found to be significantly higher in patients with schizophrenia than in controls. Leu 17 is located in the hydrophobic core region of the signal peptide. Some mutations in the hydrophobic core region of signal sequences have been reported to have a direct correlation with defective protein synthesis and pathological status. A second case-control study (560 cases, 576 controls), has been performed to test the findings of the Japanese study and confirmed the association between the mutation in the CHL1 gene region and schizophrenia in the Chinese population (Chen et al., 2005).

Two studies performed in the laboratory of Melitta Schachner on CHL1 deficient mice have identified behavioral traits and structural abnormalities in these animals that share similarities with schizophrenia phenotypes. One of these studies has shown that the prepulse inhibition (PPI) of the acoustic startle response is impaired in mice deficient in CHL1 (Irintchev et al., 2004). PPI is a measure of sensorimotor gating, i.e., the ability to control the flow of information and its impairment is a characteristic

feature of major neuropsychatric disorders, most notably schizophrenia (Perry et al., 2002). The second study has been designed to characterize the CHL1 mutant mouse with respect to morphological brain abnormalities identified in schizophrenic patients (Thilo, 2006). The analyses have indeed revealed a number of aberrations typically encountered in patients with psychosis: enlarged brain ventricles, hippocampal dysplasia, loss of inhibitory interneurons in the hippocampus and of dopaminergic neurons in substantia nigra. The conclusion from these two investigations is that the CHL1 deficient mouse shows phenotypic features which can be of value for neuropsychiatric research.

1.4.2.2 CHL1 mutations and the 3p syndrome in humans

The coding region of CHL1 gene is located on human chromosome 3p26. In humans, mutations in the CHL1 gene ortholog, former known as CALL (cell adhesion L1-like), are associated with the human 3p syndrome, caused by distal deletions of the short (p) arm of chromosome 3, and which is characterised by mental retardation or low IQ, and delayed speech and motor development (Angeloni et al., 1999; Frints et al., 2003).

Most patients with partial 3p monosomy show a contiguous gene deletion syndrome with constant clinical findings of severe mental retardation, pre- and postnatal growth retardation and facial dysmorphism. Additional clinical features include deafness, digital abnormabilities, renal and gastrointestinal abnormalities and congenital heart defects, depending on the extent of the deletion. Frints et al. (2003) hypothesize that a 50% reduction of CHL1 expression in the developing brain results in cognitive deficits in humans. This suggests that the CHL1 gene in humans at 3p26.3 is a primary candidate for an autosomal form of mental retardation. Mental retardation is also a common feature in patients with 3p and ring chromosome 3 syndromes, with breakpoints at 3p25.3 and 3p26.1 (Asai et al., 1992; Wilson et al., 1982)- respectively, suggesting that genes on 3p26 located close to the telomere may contribute to general intelligence and, when mutated, lead to mental retardation.

1.5 Schizophrenia - a neurodevelopmental disease?

The illness knows no boundaries, it occurs in all countries and within all ethnic groups. Across cultures, estimates of the lifetime prevalence of schizophrenia are around 1% (Keith et al., 1991; Kulhara & Chakrabarti, 2001; Torrey, 1987). In the

majority of cases, the onset of the illness is between the age of 18 and 35 years. Around 10 % of the schizophrenia patients commit suicide in the first ten years after the onset of the illness (Schwartz and Smith, 2004). Only 20 % to 30 % of the patients are eventually able to lead relatively normal lives, meaning they are able to live independently and maintain a job (Cancro, 1989). Some 20% to 30% continuously manifest moderate symptoms, and more than half of the patients experience life-long disability (Schwartz and Cohen, 2001).

At present, no laboratory procedure, neuroimaging method or psychological test are diagnostic of schizophrenia. The diagnosis of the illness based on the quantity, extent and durability of a large number of symptoms. Different definitions of the symptoms lead to large variability in the diagnosis of schizophrenia. Schizophrenia can be diagnosed when symptoms of the disorder have been present at least for six months. The characteristic symptom criteria for schizophrenia include positive symptoms, i.e. hallucinations, delusions, disorganized speech, grossly disorganized or catatonic behavior, and negative symptoms. The latter include altered emotional expression, poverty of speech and volition. The second group of diagnostic criteria is considered in association with evidence of social or occupational dysfunction (Walker et al., 2004).

The symptoms of schizophrenia appear to be associated with functional and structural changes in a number of neocortical regions, including heteromodal prefrontal and temporal association cortices, as well as in the connections and integrative interactions among these regions, corticolimbic areas, and the thalamus (Costa, 1998). Three general considerations regarding the etiology of schizophrenia have been emphasized over the years. The first one is that the etiology of schizophrenia involves interplay between brain vulnerability of genetic origin and environmental factors. Second, the illness does not emerge from a defect in a specific brain region but rather from a dysfunction of circuits in multiple brain regions. And finally, brain maturational processes play a critical role in the etiological process (Walker et al., 2004). The most widely accepted hypothesis for the etiology of schizophrenia is the “two-hit” hypothesis (Weinberger, 1987). According to this hypothesis, a first, gene dysfunction-related hit lays the foundation to the disease and occurs during ontogenetic development of the nervous system. This hit "labilises" the nervous system for a second hit in the perinatal or early postnatal periods (“two-hit” hypothesis) or yet other hits that occur later in life, mostly around puberty (“multiple-hit” hypothesis), such that the overt disease develops in the second or third decade of human life.

It is commonly accepted that genetic factors play a significant role in the genesis of schizophrenia. Monozygotic twins, who share nearly 100% of their genes, have the highest concordance rate for schizophrenia. Among monozygotic twins of patients with schizophrenia, 25% to 50 % will develop the illness. Dizygotic twins and other siblings share, on average, only about half of their genes. About 10 % to 15 % of dizygotic twins of patients are also diagnosed with the illness (Gottesman, 1991). Findings from genetic studies of schizophrenia have lead to the conclusion that the disorder involves multiple genes, rather than a single gene (Gottesman, 1991, 1993; Gottesman and Shields, 1976; O`Rourke, 1982, Shaw, 1998).

Several genes have been identified as potential susceptibility factors for the disease, when mutated. It is likely that combinations of the genotypes have synergistic effects on disease risk. The identified genes display functions that would fit with the neurodevelopmental hypothesis for predisposition for schizophrenia and the view that the disease arises from abnormal connectivity and synaptic functions. Among these genes is Disrupted-in-Schizophrenia 1 (DISC1) which is prominently expressed in the developing nervous system and has been found to be mutated in schizophrenia patients (Austin et al., 2004; Ma et al., 2002; Morris et al., 2003). Other candidate genes are neuregulin 1, a gene involved in multiple developmental steps, including migration of oligodendrocytes and myelin formation; dysbindin, a coiled-coil-containing protein binding to dystrobrevins and present at high expression level in hippocampal mossy fiber terminals; G72, associated with D-aminoacid oxydase; and the regulator of G-protein signaling 4 (RGS4). Aetiologically relevant is also the catechol-O-methyltransferase gene located in the velocardiofacial syndrome region on chromosome 22q11 (Harrison and Weinberger, 2005). The extracellular matrix glycoprotein reelin has also been implicated in schizophrenic symptoms, since it is down-regulated in schizophrenic patients (Tissir and Goffinet, 2003). Finally, disease susceptibility has been recently associated with genetic variation in the 8p21.3 gene, PPP3CC, encoding the calcineurin gamma subunit (Gerber et al, 2003).

The environmental risks contributing to schizophrenia are divided in prenatal and postnatal factors. The prenatal events which have been linked to increased risk for schizophrenia are, for example, maternal infection and prenatal maternal stress. Researchers have found that the risk for schizophrenia is elevated for individuals born shortly after a flue epidemic (Barr et al., 1990; Murray et al., 1992) or after being exposed to rubella (Brown et al., 2001). Prenatal maternal stress with elevated

glucocorticoid hormone levels leads to disturbances of fetal neurodevelopment and impairs the subsequent functioning of the hypothalamic-pituitary-adrenal axis (Smythe et al., 1994; Poltyrev et al., 1996; Welberg & Seckl, 2001). Prenatal or delivery complications associated with hypoxia (fetal oxygen deprivation) have been most strongly linked with later schizophrenia (Cannon, 1998, 2000). The postnatal events which have been linked with the increased risk rate for schizophrenia are postnatal brain insults and head injuries (AbdelMalik et al., 2003). It may be that the genetic vulnerability for schizophrenia involves an increased sensitivity to prenatal complications (Cannon, 1998) and/or postnatal brain trauma (AbdelMalik et al., 2003). It is uncertain whether sex is a cofounder. Greater structural abnormalities in men than in women with schizophrenia have been reported (Flaum et al., 1990; Nopoulos et al., 1997) but sex-related differences have not been found consistently (Lauriello et al., 1997).

There is no specific or unique cognitive deficit in schizophrenia. It appears that the impairment is generalized, although it seems that certain domains, like working memory, may be more impaired than others (Green et al., 2000). Functional magnet resonance imaging shows frontal and temporal hypoactivity in brains of schizophrenia patients. The frontal activity is related to the functional demands. In healthy patients, the activity rises with expanding cognitive exposure. The activity in schizophrenia patients levels off or even drops (Kindermann et al., 1997; Pearlson, 1997). Magnet resonance imaging has further revealed decreased frontal, temporal, and whole-brain volume (Lawrie and Abukmeil, 1998). More refined analyses have demonstrated reductions in the size of the thalamus and hypothalamus (Schmajuk, 2001). The most consistent finding in schizophrenia patients is the ventricular enlargement, especially increased volume of the lateral ventricles (Dennert and Andreasen, 1983). Structural brain changes precede the onset of schizophrenia. Individuals who develop schizophrenia show a decrease in the grey matter volume in the left parahippocampal, fusiform, orbitofrontal and cerebellar cortices, and the cingulate gyrus (Pantelis et al., 2003). The probable explanation for decreased cortical volume is reduced neutropil and neuronal size, rather than loss of neurons (Harrison; 1999). However, these findings are based on a small number of samples and have not been shown to be specific for schizophrenia. There is extensive evidence that gliosis is not present suggesting that schizophrenia is not associated with inflammatory processes or infection (Roberts et al., 1987). Postmortem investigations have revealed a decreased density of neurons in the

prefrontal, anterior cingulate (Benes et al 1986), entorhinal region (Falkai et al., 1988; Jakob and Beckmann, 1986), hippocampus (Falkai and Bogerts, 1986; Jeste and Lohr, 1989), medial dorsal thalamus (Pakkenberg, 1990), and nucleus accumbens (Pakkenberg, 1990) of subjects with schizophrenia. However, other studies failed to detected a lower density of neurons in the prefrontal, anterior cingulate or hippocampus (Akbarian et al., 1995; Arnold et al., 1995; Benes et al., 1991; Heckers et al., 1991) of schizophrenic subjects. Loss of interneurons in specific brain regions, such as the frontal and cingulate cortices, and the hippocampus, is one of the most consistent findings of post-mortem analyses of schizophrenic brains (Benes et al., 1991; Benes et al., 1998). These finding is of special interest since it indicates that the functional disturbances associated with schizophrenia arise from a misbalance between excitation and inhibition (Walker et al., 2002).

1.6 The Cre/loxP system for conditional gene ablation

Florin et al. (2004) showed that the Cre/loxP technology provides the opportunity for functional analyses of genes of interest. With this tool it is possible to produce a conditional loss of gene function in specific cell types such as neuronal and glial subpopulation (Rempe et al., 2006).

Cre is the 38-kDa product of the cre (cyclization recombination) gene of the bacteriophage P1 and is a site-specific DNA recombinase of the Int family. Cre recognizes a 34-bp site on the P1 genome called loxP (locus of X-over P1) and efficiently catalyzes reciprocal conservative DNA recombination between pairs of loxP sites. Cre-mediated recombination between two directly repeated loxP sites results in excision of the DNA between them as a covalently closed circle (Fig. 1). Unlike many recombinases of the Int family, no accessory host factor or DNA topological requirements are required for efficient Cre-mediated DNA recombination (Sauer, 1998).

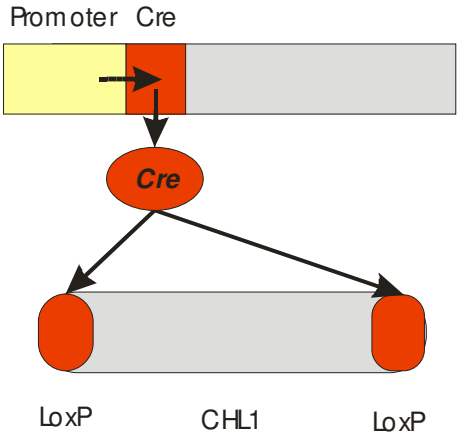

Figure 1. Principle of Cre/loxP-mediated gene ablation. Driven by a selected promoter, the Cre gene is activated resulting in synthesis of Cre recombinase. The recombinase specifically recognizes loxP sequences flanking a gene of interest, in this case CHL1, and removes that gene from the genome.

The power and spectrum of application of this system depends on transgenic mouse lines that provide Cre recombinase activity with a defined cell type, tissue, and developmental stage specificity (Novak et al., 2000). Crucial for the efficacy of the Cre/loxP system is the selection of an efficient promoter to drive the expression of Cre. Here, two promoters used in the transgenic mice analyzed in this study, the calcium/calmodulin-dependent protein kinase II promoter and the synapsin I promoter, require consideration.

1.7 Calcium/calmodulin-dependent protein kinase II

CaMKII (Calcium/calmodulin-dependent protein kinase II) is a multifunctional Ca^{2}+/calmodulin-dependent serin/threonine kinase which is able to phosphorylate a variety of proteins in response to Ca^{2+} signals. This kinase also plays an essential role in induction of long-term potentiation and neurotransmitter synthesis and release. The kinase participates in the regulation of numerous cellular functions including metabolism of carbohydrates, lipids and amino acids, regulation of ion flux through ion channels, calcium homeostasis, cytoskeletal functions and calcium regulated changes in gene expression.

There are 4 CaMKII genes (alpha, beta, gamma, and delta), and each yields several isoforms through alternative splicing. CaMKII isoforms are not uniformly expressed in time and space; the alpha and beta forms are found primarily in the nervous tissue with beta expression initiating during embryonic development and alpha

postnatally. Only the ubiquitous gamma- and delta-CaMKinaseII are expressed during early development (Bayer et al., 1999).

Sola et al. (1999) showed that CaMKII alpha mRNA is distributed in the forebrain of the mouse, mainly in the hippocampus, cerebral cortex, and striatum. CaMKII alpha mRNA is highly detected in the pyramidal cell layer of the Ammon`s horn and in the granule cell layer of the dentate gyrus of the hippocampus. A strong signal for CaMKII alpha is also detectable in the superficial layers in the cerebral cortex. The thalamus shows a very weak signal. This kinase is only expressed in excitatory neurons. All layer V neurons identified as projecting to the spinal cord are CaMKinaseII alpha immunopositive (Pinaudeau-Nasarre et al., 2002). In the hypothalamus, substanica nigra and other midbrain or brain stem structures no hybridisation signal is detectable, but strong immunoreactivity is found in the substancia nigra pars reticulata in association with axons. However, no staining is detectable in neuronal cells in pars compacta (Sola et al., 1999). CaMKII alpha is first expressed around the second week postnatal, a time point that correlates with the start of dendritic maturation and increased synapse formation. Expression of CaMKII seems to be limited to cells that are no longer dividing (Bayer et al., 1999). The CaMKII promoter has shown to be useful in combination with the Cre/loxP system for functional analyses of genes of interest expressed in the forebrain (Bukalo et al., 2004; Law et al., 2003).

1.8 Synapsin I

Synapsin I is a member of a family of nerve terminal-specific phosphoproteins consisting of two isoforms, Ia and Ib (Carola et al., 1988). Synapsin I is involved in the regulation of neurotransmitter release and is specifically expressed in neurons (Ueda and Greengard, 1977). Immunocytochemical studies have localized synapsin to the presynaptic terminals of virtually all neurons, where it is associated with the cytoplasmic surface of small synaptic vesicles (DeCamilli et al., 1983; Navone et al., 1984). However, observations at the cellular level showed high expression of synapsin mRNA in granule cells but not in their neighboring Purkinje cells (Haas and DeGennaro, 1988). Additionally, ectopic expression of a transgene under the rat synapsin I promoter has been detected in the testis in transgenic mouse lines (Street et

al., 2005). The gene encoding synapsin I is localized to the human X chromosome (Yang-Feng et al., 1986).

During development, the expression of synapsin I correlates temporally and topographically with synapse formation (Melloni and DeGennaro, 1994), and recent physiological studies (Lu et al., 1992) have suggested that synapsin I may participate in the functional maturation of synapses. The protein is phosphorylated by both cAMP-dependent and calcium/calmodulin-dependent proteinkinases, and its state of phosphorylation is altered by conditions that affect neuronal activity (Nestler and Greengard, 1984).

From the earliest embryonic time point assayed (embryonic day 12), the expression of the synapsin I gene is detectable in both the central and the peripheral nervous systems (Melloni and DeGennaro, 1994). In both regions, the onset of synapsin I gene expression correlates with the period of stem cell commitment to terminal differentiation. In a second phase, synapsin I gene expression increases to a maximum for a given neuronal population during a particular phase of differentiation, the synaptogenesis (Melloni and DeGennaro, 1994). Studies have shown that two mRNA classes with a molecular size of 3.4 and 4.5 kb translate into synapsin polypeptides. During development of the rat brain and cerebellum, the expression of the two mRNAs is differentially regulated. The expression levels of the 4.5 kb mRNA in the cerebellum decreases to a minimum after postnatal day 7. However the 3.4-kb mRNA is found also in the adult cerebellar brain with a peak in the expression at postnatal day 20. This expression pattern coincides with the period of synaptogenesis and synaptogenic differentiation in the cerebellum.

2 Rationale and aims of the study

A previous study performed in Dr. Schachner's laboratory (Thilo, 2006) on constitutive CHL1 deficient mice has shown that CHL1 deficiency causes developmental gross-anatomical abnormalities such as an age-related postnatal increase in the total brain mass and volume, enlarged brain ventricles, and hippocampal dysplasia. In addition, analyses of CHL1 deficient mice at ages of 2, 6 and 12 months revealed genotype-related alterations in the size of major neuronal and glial cell populations in areas typically affected in patients with schizophrenia such as the cortex and hippocampus. Further more, this study found evidence for abnormalities in nuclei providing dopaminergic innervation of the forebrain in CHL1 deficient mice. These findings indicate the importance of CHL1 for the development and postnatal maintenance of the brain tissue. At the same time, these results raise the question at which time points of normal brain development and maturation is CHL1 of crucial importance. This question was addressed here by using two conditional CHL1-deficient mouse lines in which the CHL1 gene is ablated using the Cre/loxP technology. In one of the mouse lines analyzed here, the Cre/loxP system was driven by the synapsin I promoter which starts to be active in all neurons in the CNS after embryonic day 12 (E12). This means that the CHL1 gene in this mouse line will be ablated during late embryogenesis and early postnatal life when synapsin I expression reaches high levels in all brain regions. In the second mouse line used, the Cre/loxP system is driven by the CaMKII promoter. It is expected that CHL1 in this mouse line occurs late during postnatal development, i.e. between 14 and 40 days of age, and is restricted to the forebrain. The aims of this study were:

-To analyze the impact of early conditional CHL1 ablation (after E13) on gross anatomical variables and defined cell populations in the hippocampus and motor cortex, areas known to be affected in adult mice constitutively deficient in CHL1 expression.

-To analyze the impact of late conditional CHL1 ablation (after the second postnatal week) on gross anatomical variables and defined cell populations in the hippocampus and motor cortex.

The methodological approached used was that described previously by Irintchev et al. (2005). This approach is based on immunohistochemical visualization of defined cell types such as, for example, total neuronal population, subpopulations of interneurons, and microglia, and stereological estimation of cell densities and volumes of structures. The analyses in this study were restricted to cell types in the hippocampus, motor cortex and substantia nigra which are affected in adult (6 to 12-month-old) constitutively CHL1-deficient mice, for example total cell density and reelin positive cell density of the motor cortex, PV positive cell density of the hippocampus or TH positive cell density of the substantia nigra (Thilo, 2006).

3 Materials and Methods

3.1 Animals

The conditional CHL1-deficient mice used in this study have been generated in Dr. Schachner's laboratory by crossing a mouse mutant carrying loxP sites in the CHL1 gene with transgenic mice that expresses the cre recombinase under the control of the CaMKII promoter (Mayford et al., 1995; Mantamadiotis et al., 2002) or the synapsin I promoter (Zuh et al., 2001). From each mouse line, both CHL1-deficient mice (CaMKII Cre+ or Syn Cre+) and wild-type littermates (CaMKII Cre- or Syn Cre-) were analyzed. All mice were bred in the specific pathogen-free utility of the Universitätsklinikum Hamburg. Treatments of the animals were performed in accordance to the German law for protection of experimental animals. All analyses were performed blindly with respect to the genotype of the animals.

3.2 Experimental design

The genotype, gender and number (N) of animals used were as follows:

Table 1 CaMKII mice studied at the age of 7 months

	CaMK Cre- (CHL1+/+) female	**CaMK Cre- (CHL1+/+) male**	**CaMK Cre+ (CHL1-/-) female**	**CaMK Cre+ (CHL1-/-) male**
N	4	3	4	3

Table 2 Synapsin I mice studied at the age of 12 months

	Syn Cre- (CHL1+/+) female	**Syn Cre- (CHL1+/+) male**	**Syn Cre+ (CHL1-/-) female**	**Syn Cre+ (CHL1-/-) male**
N	5	3	3	2

All animals were analyzed with respect to:

1. Gross-anatomical variables: brain mass, ventricular volumes, hippocampal volume and cortical thickness.
2. Densities of immunohistochemically identified cell types in the motor cortex, hippocampus, substantia nigra and amygdala.

3.3 Control of gene inactivation

3.3.1 Western blot analyses

Prior to this study, adult (3-month-old) mice from both lines were analyzed by Western blot to estimate the degree of gene inactivation using whole brain homogenates. Crude protein extract was obtained and incubated with CHL1 antibodies (R&D Systems GmbH, Wiesbaden-Nordenstadt, Germany) and horseradish peroxidase-conjugated anti-rabbit secondary antibodies (Dianova, Hamburg, Germany). Immunoreactivity was detected by enhanced chemiluminescence on x-ray film. Band intensity was quantified with densitometry (experiments performed by Andreyeva Aksana, results shown with permission). A strong reduction in the CHL1 expression level was found in Cre+ mice compared with wild-type mice (Cre-) in the CaMKII line and the Syn line (about -70% in both lines, Figs. 2 and 3).

3.3.1.1 Western blot of CaMKII Cre+ and Cre- mice

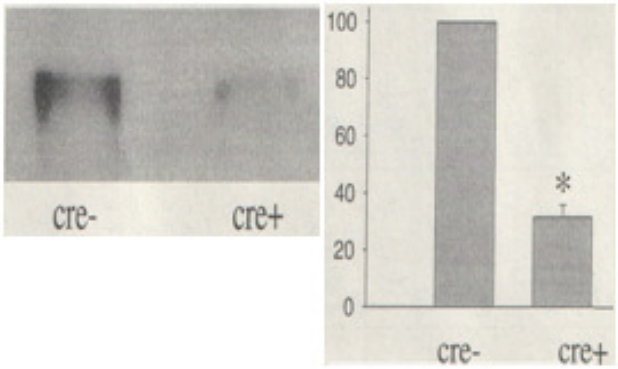

Figure 2 Western blot analysis of the CaMKII Cre- and Cre+ mice. Shown is the CHL1/synaptophysin ratio. The expression of CHL1 in relation to the expression of synaptophysin was set to 100%. The expression of CHL1 is significantly reduced in Cre+ compared with Cre- mice.

3.3.1.2 **Western blot of Syn Cre+ and Cre- mice**

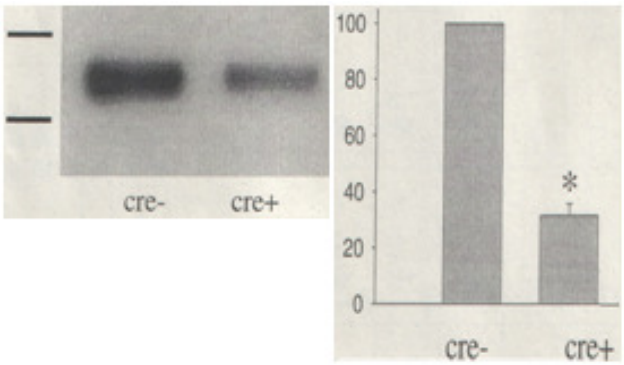

Figure 3 Western blot analysis of the Syn Cre- and Cre+ mice. Shown is the CHL1/synaptophysin ratio. The expression of CHL1 in relation to the expression of synaptopysin was set to 100%. The expression of CHL1 Cre+ is significantly reduced compared with Cre- mice.

3.4 Tissue fixation and sectioning

Tissue processing was performed as described (Irintchev et al., 2005). Mice were anaesthetized with 16% w/v (weight/volume) solution of sodium pentobarbital (Narcoren, Merial, Hallbergmoos, Germany, 5 µl g^{-1} body weight, i.p.) and transcardially perfused with 4% formaldehyde and 0.1% $CaCl_2$ in 0.1 M cacodylate buffer, pH 7.3, for 15 minutes at room temperature (RT). The brains were post-fixed overnight at 4°C in the formaldehyde solution and then immersed into 15% sucrose solution in 0.1M cacodylate buffer, pH 7.3, for two days at 4°C. Fixed and cryoprotected (sucrose-infiltrated) brains were placed in a mouse brain matrix (World Precision Instruments, Berlin, Germany) and the caudal end was cut at a defined level (1 mm from the most caudal slot of the matrix). Brain weight was then measured using a 4-digit balance. Brain volume was determined by measurement of volume displacement using a 5-ml measuring cylinder (Roth, Karlsruhe, Germany) prefilled with 4 ml sucrose/cacodylate solution (see above). Finally, the brains were frozen by immersion into 2-methyl-butane (isopentane) precooled to -30°C in the cryostat for 2 minutes and stored in liquid nitrogen until sectioned. Serial coronal sections were cut in a rostral to caudal direction from the whole brain in a cryostat (Leica CM3050, Leica Instruments, Nußloch, Germany). Sections of 25 µm thickness were collected on SuperFrost Plus glass slides (Roth). Sampling of sections was always done in a standard sequence so that 4 sections 250 µm apart were present on each slide.

3.5 Antibodies

Table 3 The following commercially available antibodies were used at optimal dilutions

Antibody	Abbre-viation	Clone	Producer	Dilution	Representative images
Anti-parvalbumin	PV	mouse mono-clonal-clone PARV-19	Sigma, Deisen-hofen, Germany	1:1000, 9.8µg/ml Ig	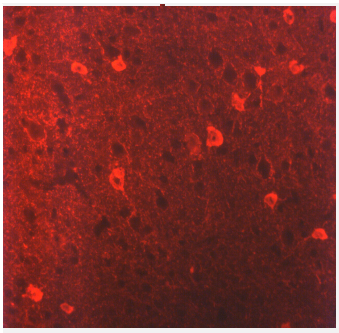
Anti-neuron specific nuclear antigen	NeuN	mouse mono-clonal-clone A60	Sigma	1:1000, 1µg/ml Ig	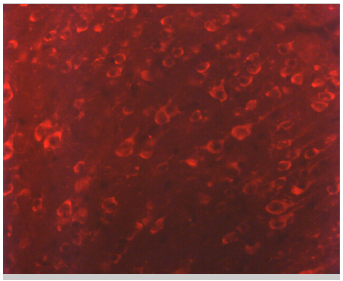
Anti-tyrosine hydroxylase	TH	Poly-clonal, affinity purified	Chemicon, Hofheim, Germany	1:750, 0.1µg/ml Ig	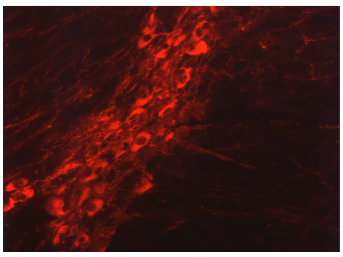
Anti-reelin	reelin	mouse mono-clonal-clone G 10, purified immune-globulin	Chemicon	1:500, 2 µg/ml Ig	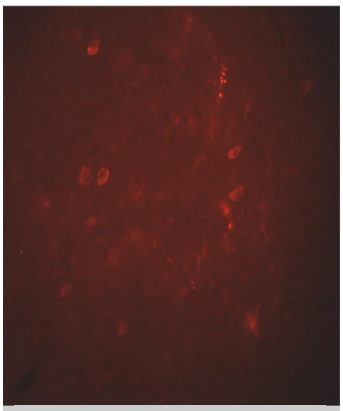

Anti-Iba1	Iba1	rabbit poly-clonal, affinity purified	Wako Chemical, Neuss, Germany	1:1500, 0.3µg/ml Ig	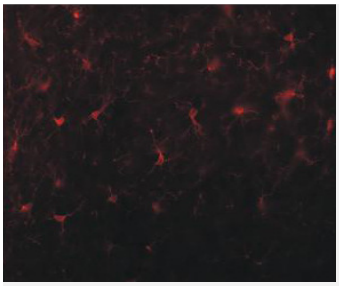
Anti-CHL1	CHL1	Goat poly-clonal, affinity purified	R&D Systems, Wies-baden, Germany	1:100, 2µg/ml IgG	See Figs. 23 and 40

Defined cell populations in studied brain regions express specific cell-marker antigens which can be detected by the used antibodies (Irintchev et al., 2004).

Parvalbumin (PV) is expressed in the neocortex and hippocampus by the major subpopulation of GABAergic neurons. It is a low molecular weight calcium-binding protein.

Neuron specific antigen (NeuN) is a protein of unknown function which is expressed nearly in all neurons in the adult brain with the exception of Purkinje, mitral and photoreceptor cells which are not found in the cerebral cortex and the hippocampus (Wolf et al., 1996).

Tyrosin hydroxylase (TH) is the rate-limiting enzyme in the synthesis of the catecholamine neurotransmitters dopamine, epinephrine and norepinephrine.

Reelin (reelin) is expressed by interneurons which do not express parvalbumin (Pesold et al., 1999)

Iba1 is involved in the activation of quiescent microglial cells. It is a calcium-binding protein, specific for microglia/macrophages (Imai and Kohsaka, 2 002).

3.6 Immunohistochemistry

Immunohistochemistry was performed as described previously (Irintchev et al., 2005). Antigen retrieval was performed by incubating the sections in 10 mM sodium citrate solution (pH 9.0) at 80°C for 30 minutes in a water bath (Jiao et al., 1999). Unspecific binding was blocked by incubation of the sections for one hour at RT in

phosphate-buffered saline (PBS, pH 7.3) containing 0.2 % v/v Triton X-100 (Fluka, Buchs, Germany), 0.02 w/v sodium azide (Merck, Darmstadt, Germany) and 5 % v/v normal goat serum (Jackson ImmunoResearch Laboratories, Dianova, Hamburg, Germany). Thereafter, the sections were incubated with the primary antibody diluted in PBS containing 0.5% w/v lambda-carrageenan (Sigma) and 0,02% w/v sodium azide in PBS for 3 days at 4°C in plastic screw cap staining jars. Following washing in PBS (3 x 15 minutes), the sections were incubated with an appropriate Cy3-conjugated secondary antibody (Jackson ImmunoResearch) diluted in PBS-carrageenan (1:200) for 2 hours at RT. After a subsequent wash in PBS, cell nuclei were stained for 10 minutes at room temperature with bis-benzimide solution (Hoechst dye 33258, 5 µg ml^{-1} in PBS, Sigma). Finally, the sections were washed again and mounted under coverslips with Fluoromount G (Southern Biotechnology Associates, Biozol, Eching, Germany). For each antigen, specificity of staining was tested by omitting the first antibody or replacing it by different concentrations of appropriate normal serum or IgG.

3.7 Stereological analyses

The optical disector principle was used to estimate cell densities as described (Irintchev et al., 2005). The counts were performed directly under an Axioskop microscope (Zeiss, Oberkochen, Germany) equipped with a motorized stage and Neurolucida software-controlled computer system (MicroBrightField Europe, Magdeburg, Germany). The motor cortical areas M1 and M2 (Franklin and Paxinos, 1997) as well as the subdivisions of the hippocampus were identified and delineated on the basis of the nuclear staining pattern seen at low-power magnification (10x objective) as described (Irintchev et al., 2005; Nikonenko et al., 2006). The numerical densities were estimated by counting nuclei of labeled cells within systematically randomly spaced optical disectors. The parameters for this analysis were: guard space depth 2 µm, base and height of the disector 3600 $µm^2$ and 10 µm, respectively, distance between the optical disectors 60 µm, objective 40x Plan-Neofluar® 40x/0.75. The same parameters were used for the counting of nuclei in the pyramidal layer except for the base of the disector and the space between disectors which were 625 $µm^2$ and 25 µm, respectively. Left and right cortical and hippocampal areas were evaluated in 4 sections each. All results shown are averaged bilateral values.

3.8 Morphometric analyses

3.8.1 Ventricular volumes

To calculate the ventricular volumes, the Cavalieri method was used. This is the most commonly used method of the estimation of a reference volume (Howard and Reed, 1998). For this, a series of systematic sections of a constant distance (T) have to be performed of the object of interest. The volume (V) can now be estimated by measuring the area (A) of the transect through the object on each section.

Est1 $V = T (A1+A2+A3+.....+Am)$

The Axioskop microscope (Zeiss, objective 10x) and a Neurolucida software-controlled computer system was used to measure the area of each ventricle transect.

3.8.2 Cortical thickness

To differentiate the agranular motor and the granular sensory cortex, the nuclear staining was used. 25µm sections cut 3-4mm caudally of the rostral pol were used. The Axiskop microscope and Neurolucida software were used to measure the area of each cortical field and the lengths of its surface boundary. The mean cortical thickness was calculated by dividing the area of the lengths of the superficial boundary.

3.8.3 Hippocampus

Using the Neurolucida system, measurements of the areas of the whole hippocampal formation, the pyramidal cell layer (CA1-3), and the granular cell layer of the dentate gyrus were performed. Areas were measured in every animal bilaterally in three coronal nuclear stained sections. The mouse brain atlas of Sidman et al. (1971) was used for the selection of the mid-section (bregma-2.10mm). Respectively 250µm rostral and caudal from the midsections were the other two counted sections. The average of the calculated areas was used to calculate individual mean value.

3.8.4 Photographic documentation

Photograpic documentation was made on an Axiophot 2 microscope equipped with a digital camera AxioCam HRC and AxioVision software (Zeiss) at highest resolution (1300 x 1030 pixel RGB). The images were processed using Adobe Photoshop 6.0 software (Adobe Systems Inc., San Jose, California).

3.9 Statistical analyses

Mean values were compared using two-sided *t* test for independent samples. The accepted level of significance was 5%. All data are presented as mean values with standard deviations.

4 Results

4.1 Analyses of mice with postnatal ablation of CHL1 (CaMK Cre+ mice)

4.1.1 Morphometric analysis of gross-anatomical variables

4.1.1.1 Brain mass

The brain mass (Fig. 4) of 7-month-old CaMK Cre+ mice did not differ from that of CaMK Cre- littermates.

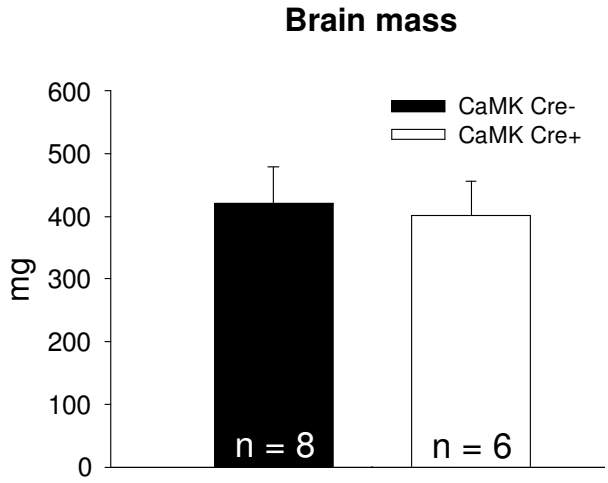

Figure 4 Brain mass of CaMK Cre- mice (black bar) and CaMK Cre+ littermates (white bar). Shown are mean values + SD. Number of animals studied per group (n) are indicated. No significant difference was found ($p > 0.05$, t test).

4.1.1.2 **Ventricular volumes**

The ventricular volume of 7-month-old CaMK Cre- animals, estimated separately for the lateral ventricles and the third ventricle, did not differ from that of CaMK Cre+ littermates (Figs. 5 and 6).

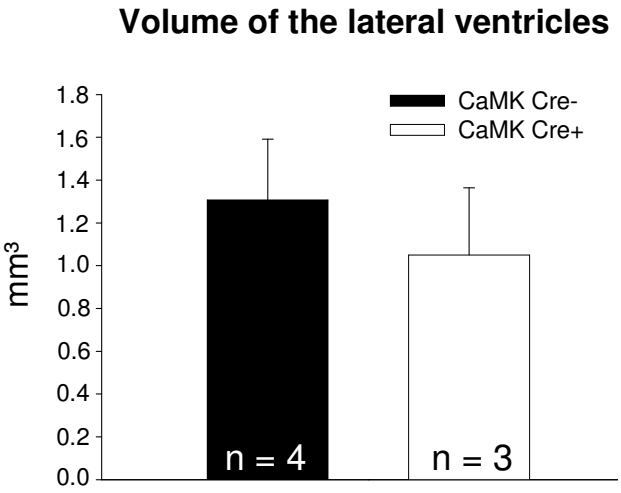

Figure 5 Volume of the lateral ventricular system of CaMK Cre- mice (black bar) and CaMK Cre+ littermates (white bar). Shown are mean values + SD. Numbers of animals studied per group (n) are indicated. No significant difference was found ($p > 0.05$, t test).

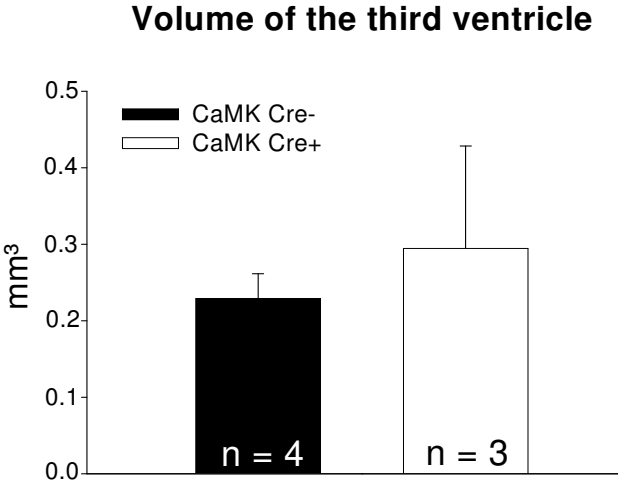

Figure 6 Volume of the third ventricle of CaMK Cre- mice (black bar) with CaMK Cre+ littermates (white bar). Numbers of animals studied per group (n) are indicated. Shown are mean values + SD. No significant difference was found ($p > 0.05$, t test).

4.1.2 **Stereological analysis of the motor cortex of CaMKII Cre+ mice**

4.1.2.1 **Thickness of the motor cortex**

The cortical thickness of 7-month-old CaMK Cre- animals was found to be significantly increased compared to that of CaMK Cre+ age-matched animals (Fig. 7).

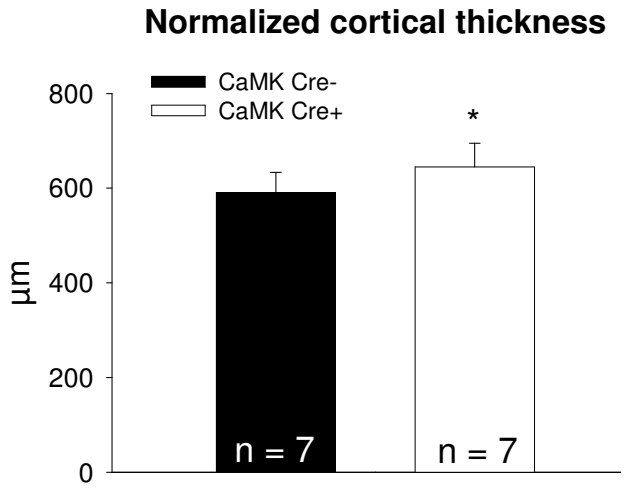

Figure 7 Thickness of the motor cortex in CaMK Cre- mice (black bar) and CaMK Cre+ littermates (white bar). Numbers of animals studied per group (n) are indicated. Shown are mean values + SD. The cortical thickness of CaMK Cre+ mice was significantly increased compared to CaMK Cre- littermates ($p < 0.05$, t test).

4.1.2.2 **Total cell density of the motor cortex**

The total cell density in the motor cortex of CaMK Cre- and CaMK Cre+ mice was similar at the age of 7 months (Fig. 8)

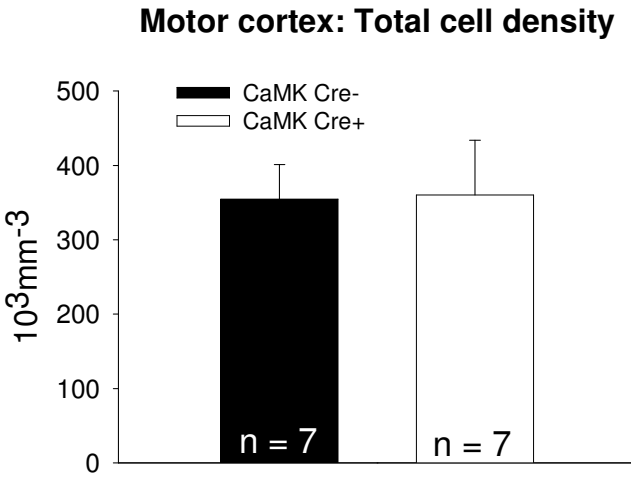

Figure 8 Total cell density in the motor cortex of CaMK Cre- mice (black bar) and CaMK Cre+ littermates (white bar). Numbers of animals studied per group (n) are indicated. Shown are mean values + SD. No significant difference was found ($p > 0.05$, t test).

4.1.2.3 **Density of NeuN-positive cells of the motor cortex**

The density of all neurons (NeuN-positive) in the motor cortex of CaMK Cre+ mice was significantly increased compared to CaMKII Cre- littermates (Fig. 9).

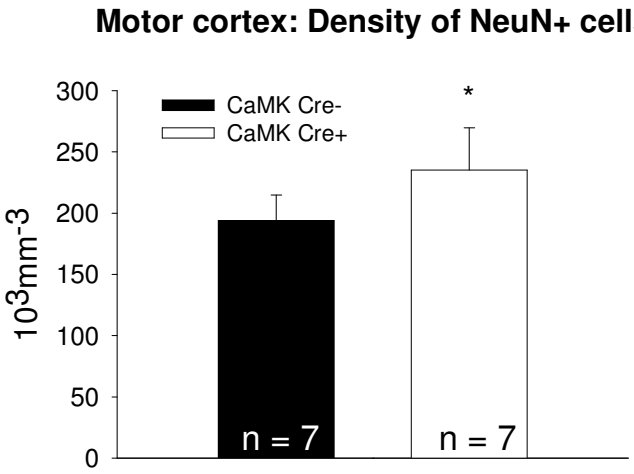

Figure 9 Density of NeuN+ cells in the motor cortex of CaMK Cre- mice (black bar) and CaMK Cre+ littermates (white bar). Numbers of animals studied per group (n) are indicated. Shown are mean values + SD. NeuN-positive cell density found to be significantly increased in the motor cortex of CaMK Cre+ mice, as compared to Cre- littermates ($p < 0.05$, t test).

4.1.2.4 **Density of PV-positive cells of the motor cortex**

No statistically significant difference was found in the number of PV-positive interneurons in Cre+ mutant animals compared to Cre- control animals (Fig. 10).

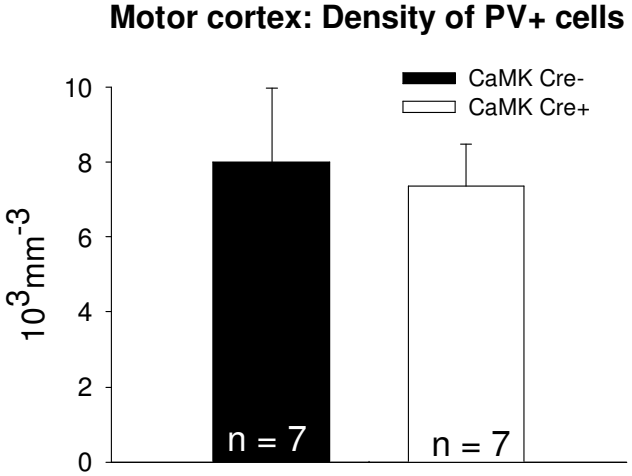

Figure 10 Density of PV+ cells in the motor cortex of CaMK Cre- mice (black bar) with CaMK Cre+ littermates (white bar). Numbers of animals studied per group (n) are indicated. Shown are mean values + SD. No significant difference was found ($p > 0.05$, t test).

4.1.2.5 **Density of reelin-positive cells of the motor cortex**

No statistically significant difference was found in the number of reelin-positive interneurons in Cre+ mutant animals compared to Cre- control animals (Fig. 11).

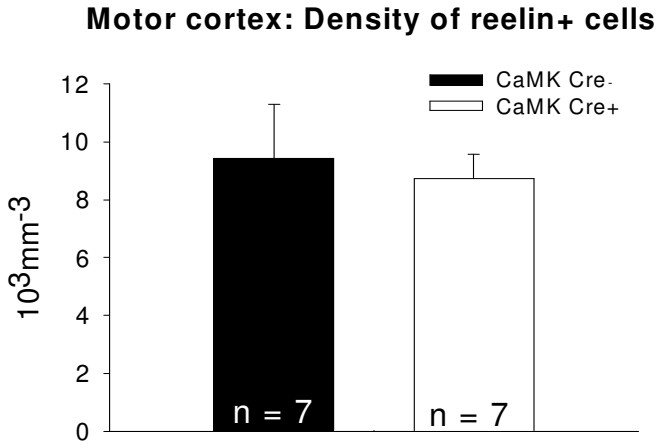

Figure 11 Density of reelin+ cells in the motor cortex of CaMK Cre- mice (black bar) and CaMK Cre+ littermates (white bar). Numbers of animals studied per group (n) are indicated. Shown are mean values + SD. No significant difference was found ($p > 0.05$, t test).

4.1.2.6 **Density of Iba1-positive cells of the motor cortex**

The results of the quantitative analysis of Iba1-positive cells revealed a similar number of microglial cells in 7-month-old CaMK Cre+ compared to control animals (Fig. 12).

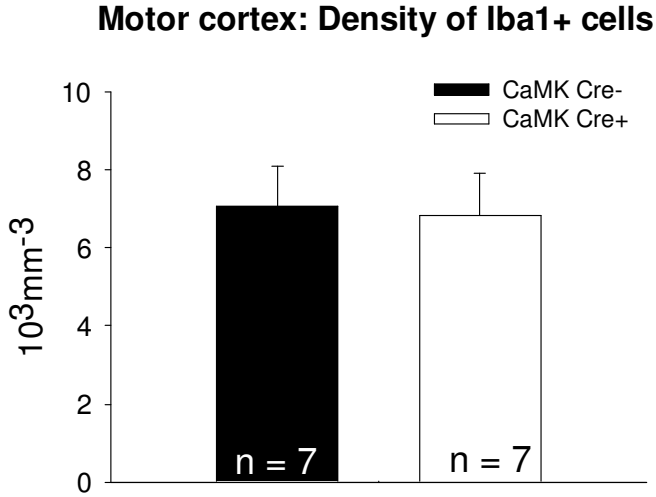

Figure 12 Density of Iba1+ cells in the motor cortex of CaMK Cre- mice (black bar) and CaMK Cre+ littermates (white bar). Numbers of animals studied per group (n) are indicated. Shown are mean values + SD. No significant difference was found ($p > 0.05$, t test).

4.1.3 **Stereological analysis of the hippocampus of CaMKII Cre+ mice**

4.1.3.1 **Area of the hippocampus, gyrus dentatus and stratum pyramidale hippocampi**

The total area of the hippocampus (Fig. 13), the area of the pyramidal layer (Fig. 14), and the area of the granular layer of the dentate gyrus (Fig. 15) were similar in CaMK Cre+ mice and Cre- littermates indicating normal size of these structures in mutant animals.

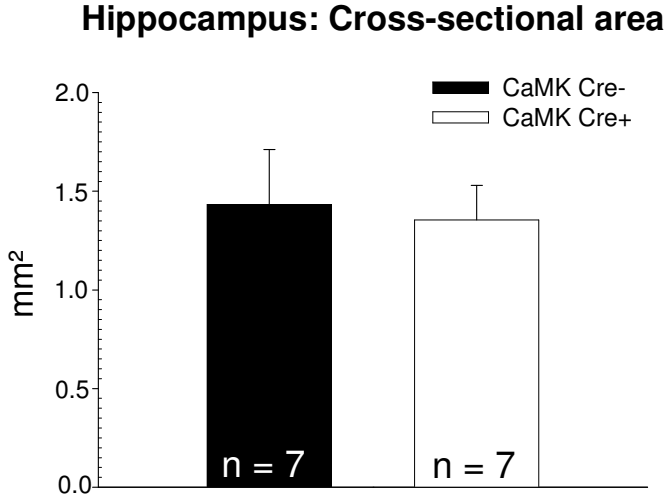

Figure 13 Total cross-sectional area of the hippocampus in coronal brain sections of CaMK Cre- mice (black bar) and CaMK Cre+ littermates (white bar). Numbers of animals studied per group (n) are indicated. Shown are mean values + SD. No significant difference was found (p > 0.05, t test).

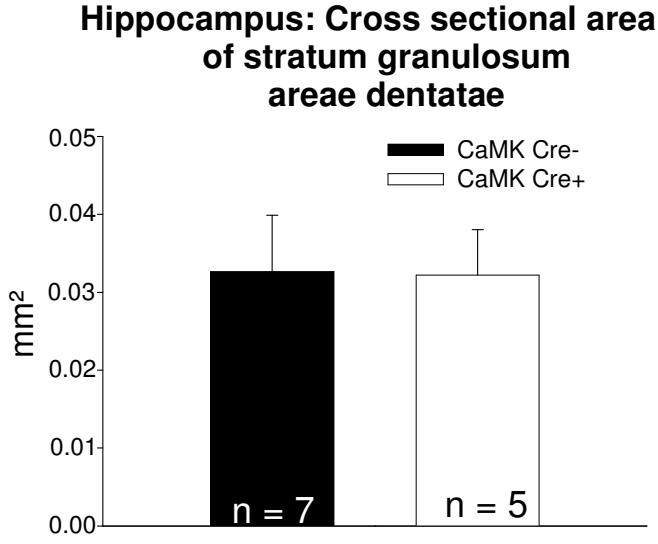

Figure 14 Total cross-sectional area of the granular layer in the dentate gyrus in coronal brain sections of CaMK Cre- mice (black bar) and CaMK Cre+ littermates (white bar). Numbers of animals studied per group (n) are indicated. Shown are mean values + SD. No significant difference was found (p > 0.05, t test).

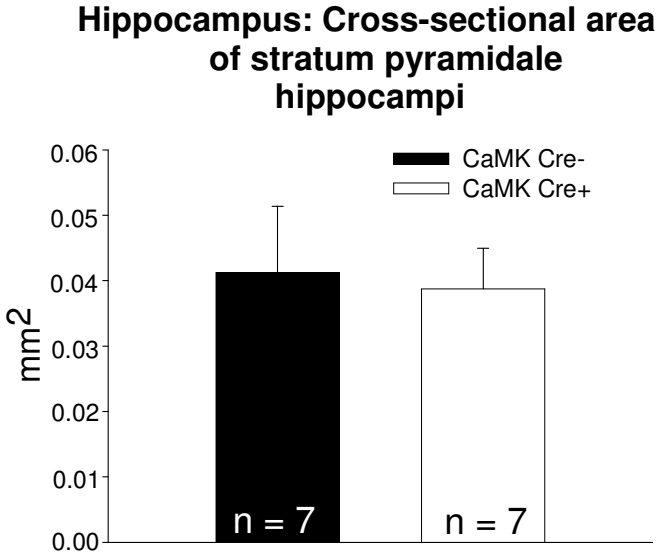

Figure 15 Total cross-sectional area of the pyramidale cell layer in coronal brain sections of CaMK Cre- mice (black bar) and CaMK Cre+ littermates (white bar). Numbers of animals studied per group (n) are indicated. Shown are mean values + SD. No significant difference was found (p > 0.05, t test).

4.1.3.2 **Density of PV-positive cells of the hippocampus**

The conditional CHL1 deficiency did not appear to affect the parvalbumin interneurons in the hippocampus (Fig. 16).

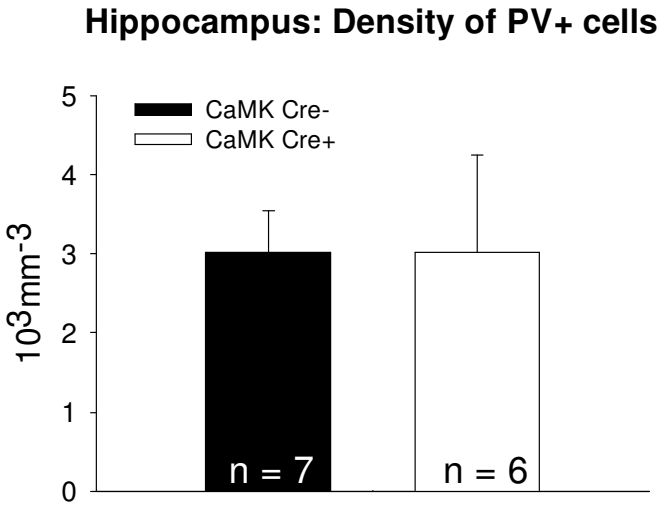

Figure 16 Density of PV+ cells in the hippocampus of CaMK Cre- mice (black bar) and CaMK Cre+ littermates (white bar) Numbers of animals studied per group (n) are indicated. Shown are mean values + SD. No significant difference was found (p > 0.05, t test).

4.1.3.3 **Density of Iba1-positive cells of the hippocampus**

The density of microgial cells in CaMK Cre+ mice was similar to that in their Cre- littermates (Fig. 17).

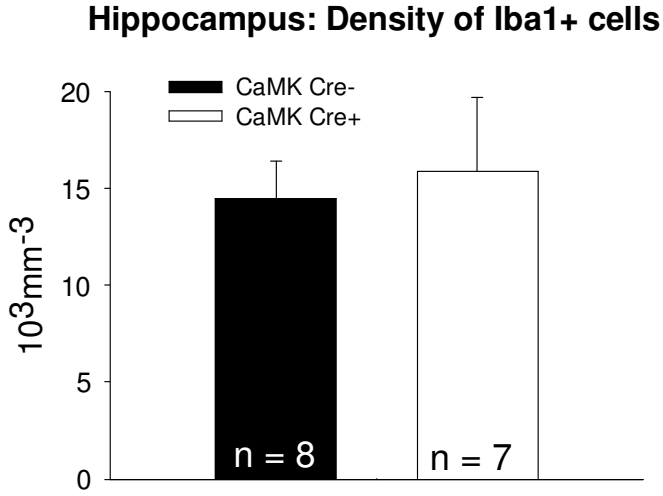

Figure 17 Density of Iba1+ cells in the hippocampus of CaMK Cre- mice (black bar) and CaMK Cre+ littermates (white bar). Numbers of animals studied per group (n) are indicated. Shown are mean values + SD. No significant difference was found ($p > 0.05$, t test).

4.1.3.4 **Total cell density of stratum pyramidale hippocampi**

The total cell density in stratum pyramidale hippocampi in the CA1 subfield, estimated by counting bis-benzimide-stained cell nuclei, revealed no difference between CaMK Cre+ and CaMK Cre- mice (Fig. 18).

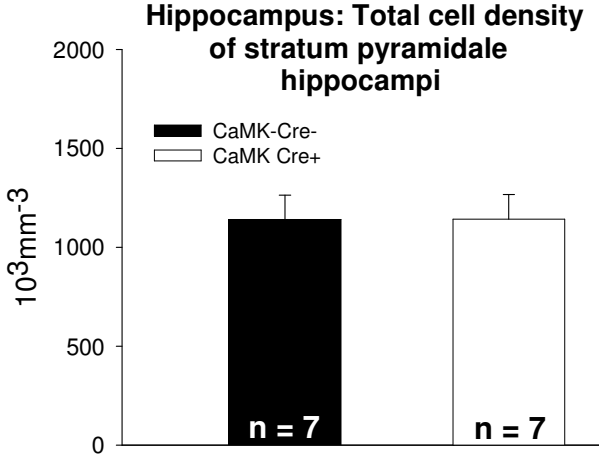

Figure 18 Density of all cells in stratum pyramidale hippocampi of the CA1 region of CaMK Cre- mice (black bar) and CaMK Cre+ littermates (white bar). Numbers of animals studied per group (n) are indicated. Shown are mean values + SD. No significant difference was found ($p > 0.05$, t test).

4.1.4 **Stereological analysis of the substantia nigra of CaMKII Cre+ mice**

4.1.4.1 **Density of TH positive cells in substantia nigra, pars compacta**

The estimation of numerical densities of dopaminergic (tyrosin hydroxylase-positive) cells revealed no significant differences between CaMK Cre+ and Cre- littermates (Fig.19).

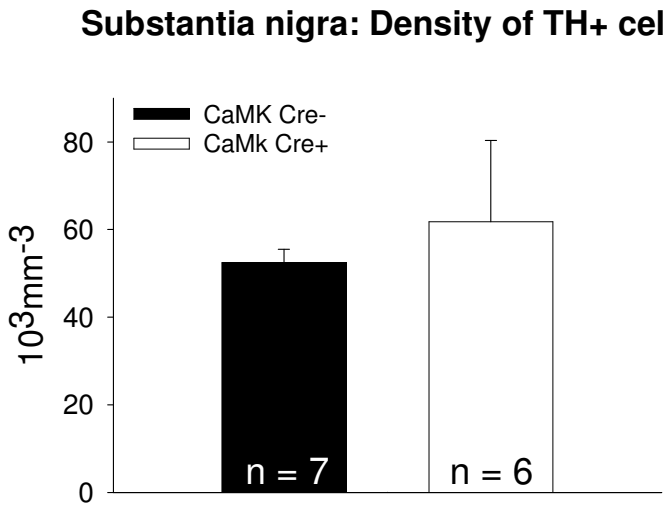

Figure 19 Density of TH+ cells in substantia nigra of CaMK Cre- mice (black bar) and CaMK Cre+ littermates (white bar). Numbers of animals studied per group (n) are indicated. Shown are mean values + SD. No significant difference was found ($p > 0.05$, t test).

4.1.5 **Stereological analysis of the amygdala of CaMKII Cre+ mice**

Investigations of cell populations in the amygdala showed no differences in the total cell density (Fig. 20), the neuronal cell density (Fig. 21) or the parvalbumin-positive cell density (Fig. 22) in CaMK Cre+ mice compared with Cre- littermates.

4.1.5.1 **Total cell density in the amygdale**

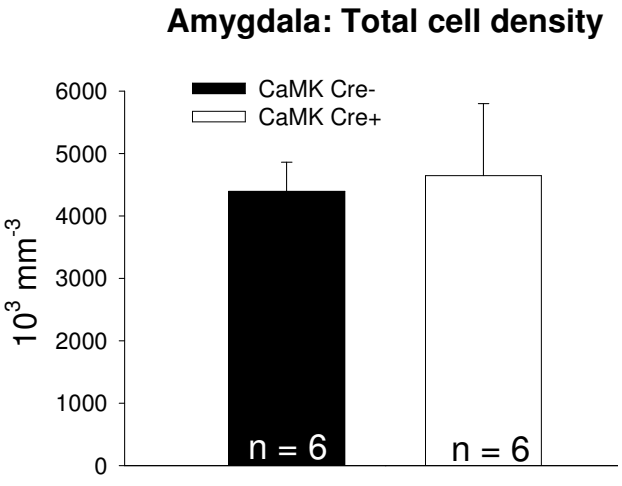

Figure 20 Total cell density in the amygdala of CaMK Cre- mice (black bar) and CaMK Cre+ littermates (white bar). Numbers of animals studied per group (n) are indicated. Shown are mean values + SD. No significant difference was found ($p > 0.05$, t test).

4.1.5.2 **Density of NeuN+ cells in the amygdale**

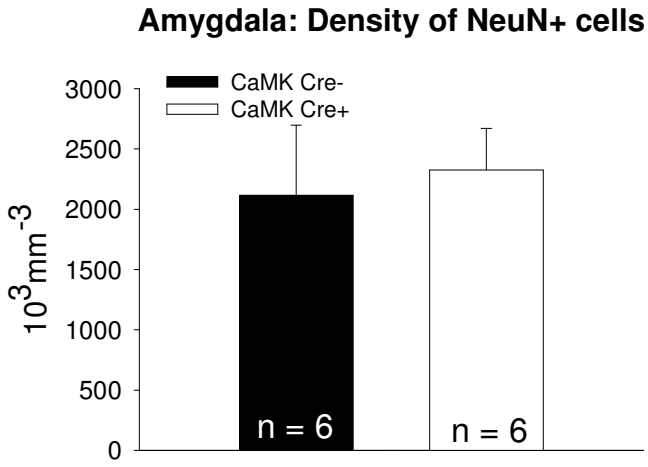

Figure 21 Density of NeuN+ cells in the amygdala of CaMK Cre- mice (black bar) and CaMK Cre+ littermates (white bar). Numbers of animals studied per group (n) are indicated. Shown are mean values + SD. No significant difference was found (p > 0.05, t test).

4.1.5.3 **Density of PV-positive cells in the amygdala**

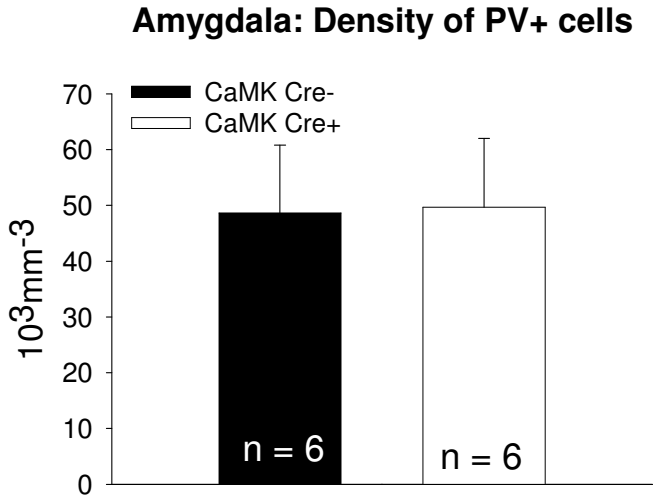

Figure 22 Density of PV+ cells in the amygdala of CaMK Cre- mice (black bar) and CaMK Cre+ littermates (white bar). Numbers of animals studied per group (n) are indicated. Shown are mean values + SD. No significant difference was found (p > 0.05, t test).

4.1.6 **Immunohistochemical analysis of CHL1 expression**

To verify that the conditional CHL1 ablation has been effective in the cortex and the hippocampus, sections from all CaMK Cre+ and CaMK Cre- mice analyzed morphologically were stained with a CHL1-specific antibody. The immunofluorescence staining revealed strong reduction of CHL1 expression in the hippocampus and neocortex in CaMK Cre+ mice compared with wild-type littermates (Fig. 23).

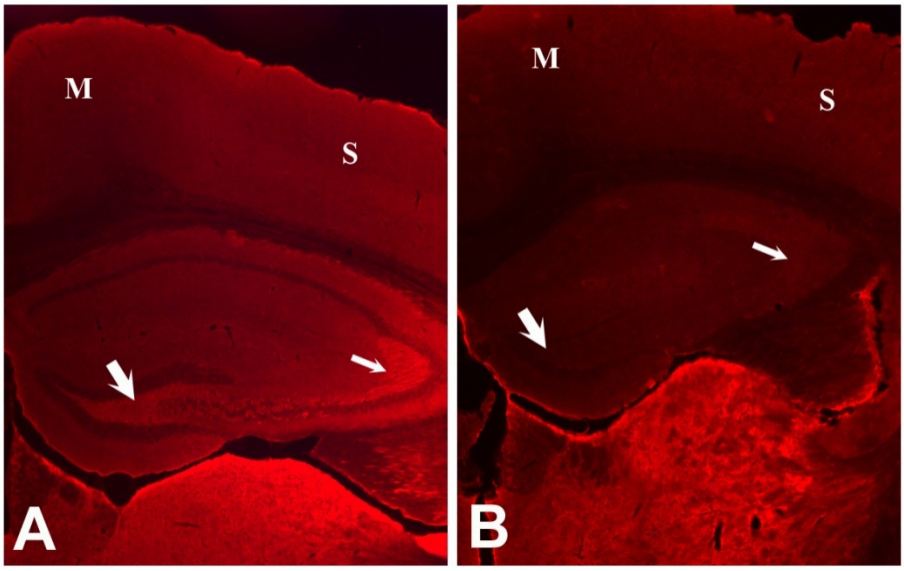

Figure 23 Immunofluorescence detection of CHL1 in representative coronal sections from a CaMK Cre- (A) and a CaMK Cre+ (B) mouse. In the CaMK Cre+ mouse (B), immunostaining is reduced, compared with CaMK Cre- mouse, in motor (M) and sensory (S) areas of the neocortex and the hippocampal formation. The thick and thin arrows point to the hilus of the dentate gyrus and stratum licidum of CA3, respectively, areas of prominent CHL1 expression in wild-type mice. Note prominent CHL1 expression ventral to the hippocampus in both genotypes.

4.2 Analyses of mice with embryonic ablation of CHL1 (Syn Cre+ mice)

4.2.1 Morphometric analysis of gross-anatomical variables

4.2.1.1 Brain mass

The brain mass of 12-month-old Syn Cre+ animals did not differ from that of Cre+ age matched animals (Fig. 24).

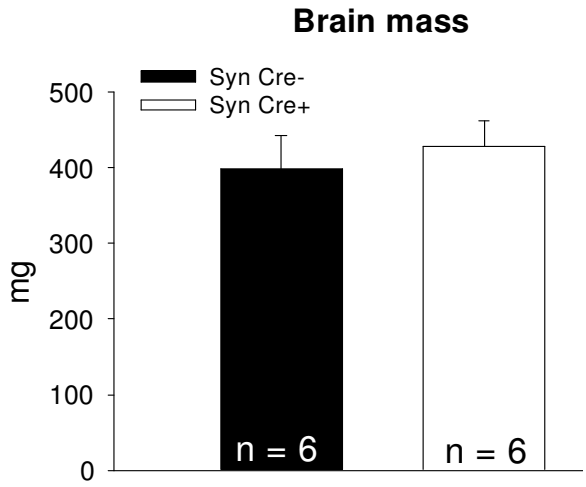

Figure 24 Brain mass of Syn Cre- mice (black bar) and Syn Cre+ (white bar) littermates. Numbers of animals studied per group (n) are indicated. Shown are mean values + SD. No significant difference was found ($p > 0.05$, t test).

4.2.1.2 Ventricular volumes

Volumetric analysis revealed a significant increase of the volume of the lateral ventricles (Fig. 25) and the third ventricle in Syn Cre+ compared with Syn Cre- mice.

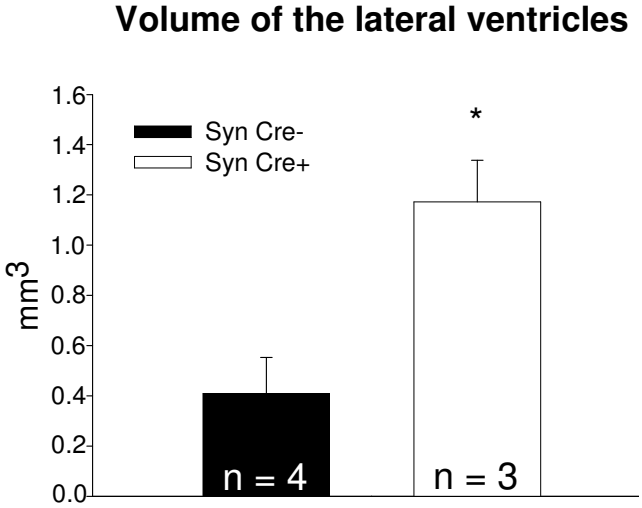

Figure 25 Volume of the lateral ventricular system of Syn Cre- mice (black bar) and Syn Cre+ littermates (white bars). Numbers of animals studied per group (n) are indicated. Shown are mean values + SD. The volume of the lateral ventricular system of Syn Cre+ mice were significantly increased, as compared with Cre- littermates ($p < 0.05$, t test).

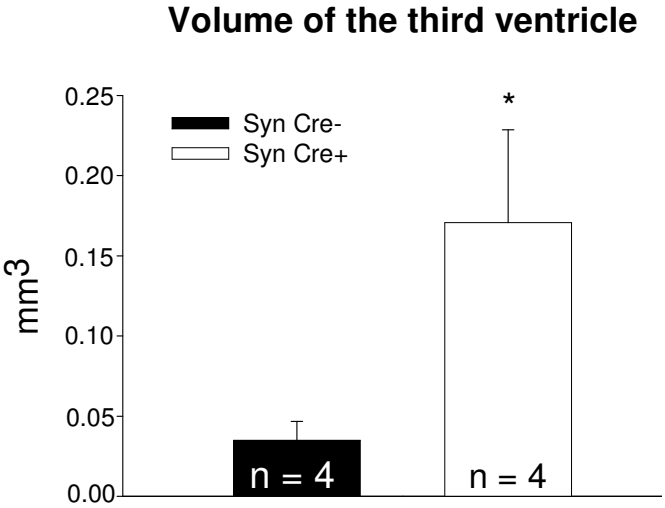

Figure 26 Volume of the third ventricle of Syn Cre- mice (black bar) and Syn Cre+ littermates (white bars). Numbers of animals studied per group (n) are indicated. Shown are mean values + SD. The volume of the third ventricle of Syn Cre+ mice was significantly increased as compared with Syn Cre- littermates ($p < 0.05$, t test).

4.2.2 **Stereological analysis of the motor cortex of Syn Cre+ mice**

The thickness of the motor cortex was similar in Syn Cre+ mice and their wild type littermates (Fig. 27). No differences between the genotypes were also found for total cell density (Fig. 28), density of NeuN-positive cells (Fig. 29), and densities of parvalbumin-positive cells (Fig. 30), reelin-positive interneurons (Fig. 31) and Iba1-positive cells (Fig. 32).

4.2.2.1 **Cortical thickness of the motor cortex**

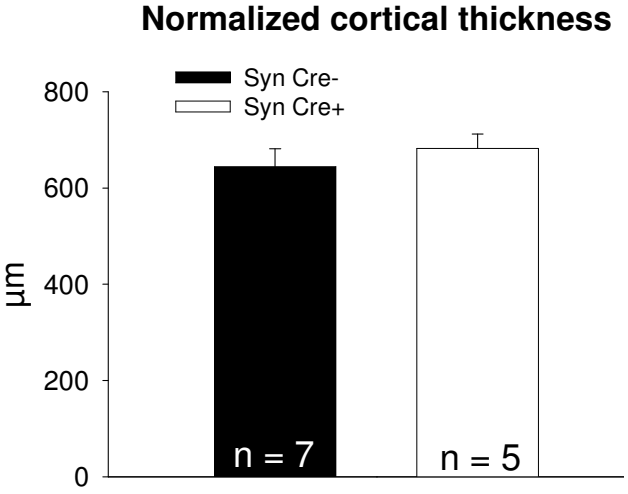

Figure 27 Thickness of the motor cortex in CaMK Cre- mice (black bar) and CaMK Cre+ littermates (white bar). Numbers of animals studied per group (n) are indicated. Shown are mean values + SD. No significant difference was found ($p > 0.05$, t test).

4.2.2.2 **Total cell density of the motor cortex**

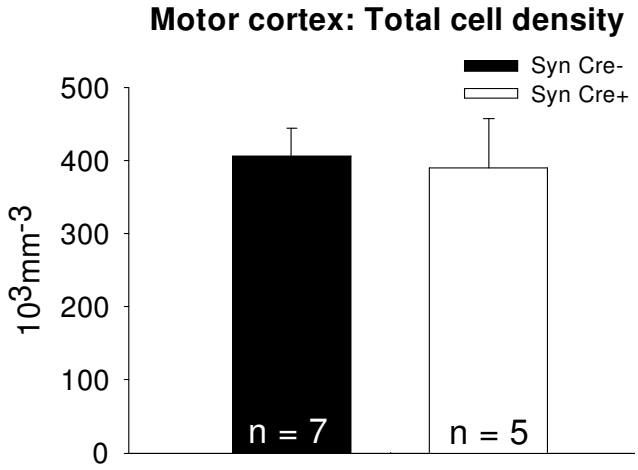

Figure 28. Total cell density in the motor cortex of Syn Cre- mice (black bar) and Syn Cre+ littermates (white bar). Numbers of animals studied per group (n) are indicated. Shown are mean values + SD. No significant difference was found ($p > 0.05$, t test).

4.2.2.3 **Density of NeuN-positive cells of the motor cortex**

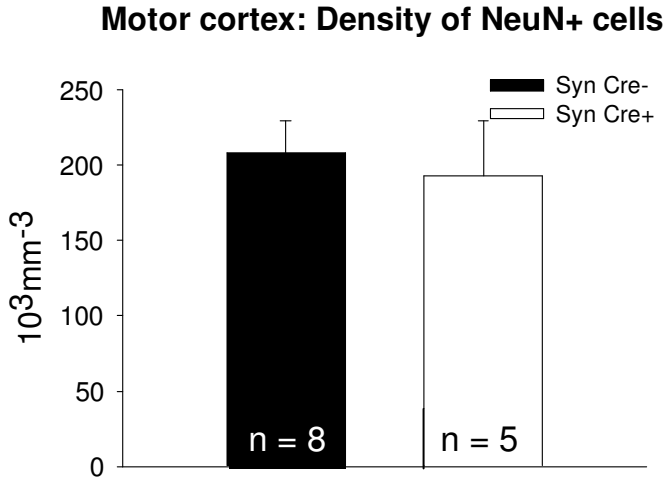

Figure 29 Density of NeuN+ cells in the motor cortex of Syn Cre- mice (black bar) and Syn Cre+ littermates (white bar). Numbers of animals studied per group (n) are indicated. Shown are mean values + SD. No significant difference was found ($p > 0.05$, t test).

4.2.2.4 **Density of PV-positive cells of the motor cortex**

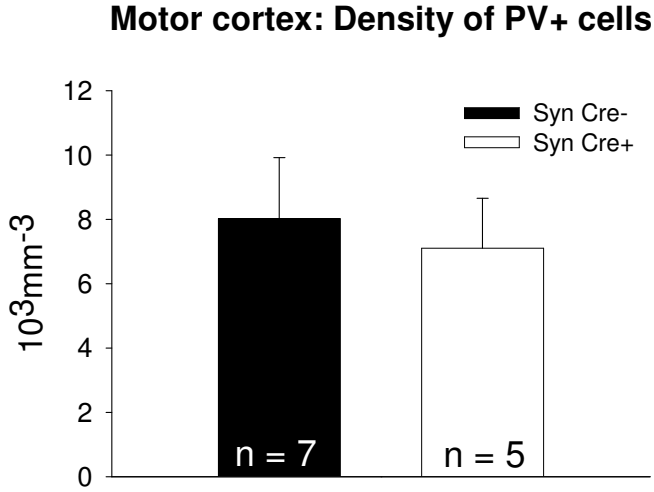

Figure 30 Density of PV+ cells in the motor cortex of Syn Cre- mice (black bar) and Syn Cre+ littermates (white bar). Numbers of animals studied per group (n) are indicated. Shown are mean values + SD. No significant difference was found ($p > 0.05$, t test).

4.2.2.5 **Density of reelin-positive cells of the motor cortex**

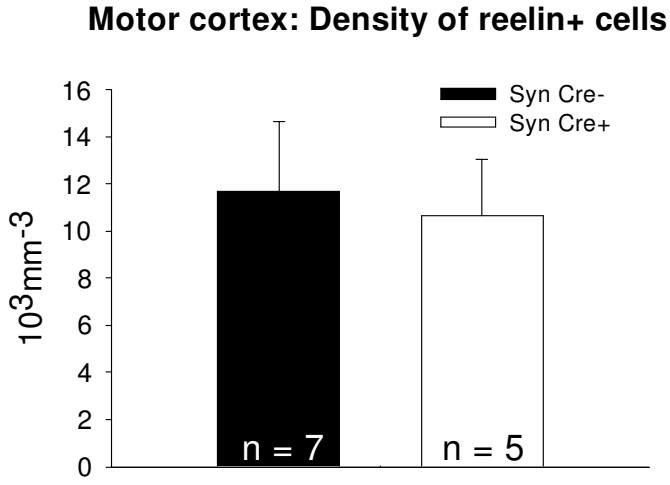

Figure 31 Density of reelin+ cells in the motor cortex of Syn Cre- mice (black bar) and Syn Cre+ littermates (white bar). Numbers of animals studied per group (n) are indicated. Shown are mean values + SD. No significant difference was found ($p > 0.05$, t test).

4.2.2.6 **Density of Iba1-positive cells of the motor cortex**

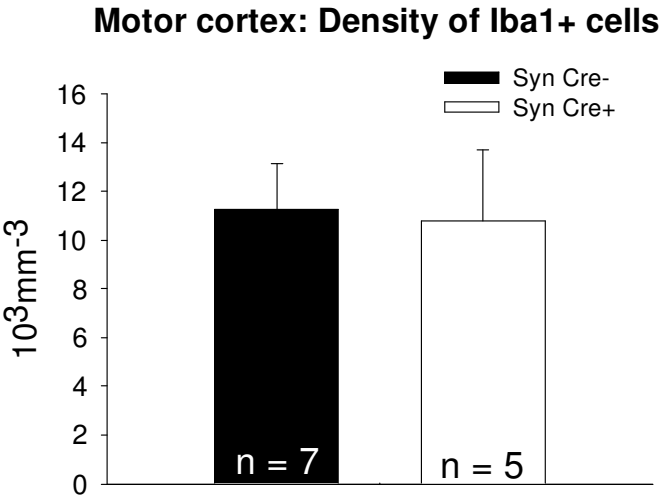

Figure 32. Density of Iba1+ cells in the motor cortex of Syn Cre- mice (black bar) and Syn Cre+ littermates (white bar). Numbers of animals studied per group (n) are indicated. Shown are mean values + SD. No significant difference was found (p > 0.05, t test).

4.2.3 **Stereological analysis of the hippocampus of Syn Cre+ mice**

4.2.3.1 **Area of the hippocampus**

No differences were observed for the total area of the hippocampus (Fig. 33), the area of the granule cell layer of the dentate gyrus (Fig. 34) or the area of the stratum pyramidale hippocampi (Fig. 35) in Syn Cre+ animals compared to Syn Cre- littermates.

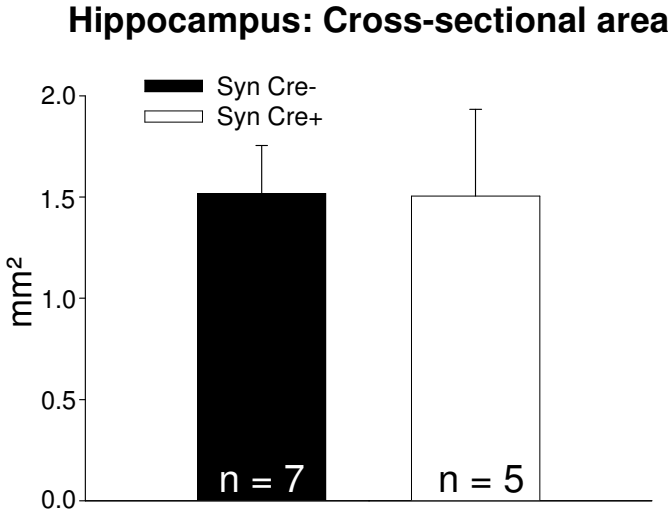

Figure 33 Total cross-sectional area of the hippocampus in coronal brain sections of the dorsal hippocampus of Syn Cre- mice (black bar) and Syn Cre+ littermates (white bar). Numbers of animals studied per group (n) are indicated. Shown are mean values + SD. No significant difference was found (p > 0.05, t test).

4.2.3.2 **Area of stratum dentati hippocampi**

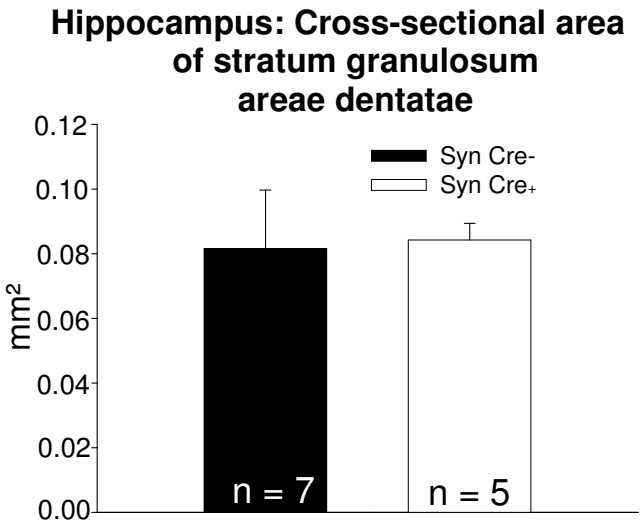

Figure 34 Cross-sectional area of the granular layer in the dentate gyrus in coronal brain sections of Syn Cre- mice (black bar) and Syn Cre+ littermates (white bar). Numbers of animals studied per group (n) are indicated. Shown are mean values + SD. No significant difference was found ($p > 0.05$, t test).

4.2.3.3 **Area of the pyramidal cell layer**

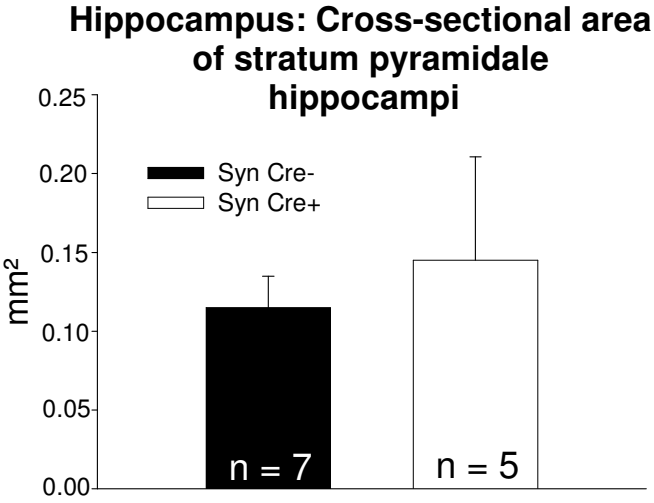

Figure 35 Total cross-sectional area of the pyramidal cell layer in the CA1 region in coronal brain sections of Syn Cre- mice (black bar) and Syn Cre+ littermates (white bar). Numbers of animals studied per group (n) are indicated. Shown are mean values + SD. No significant difference was found ($p > 0.05$, t test).

4.2.3.4 **Density of PV-positive cells of the hippocampus**

The conditional CHL1 deficiency did not appear to affect the parvalbumin interneurons in the hippocampus (Fig. 36)

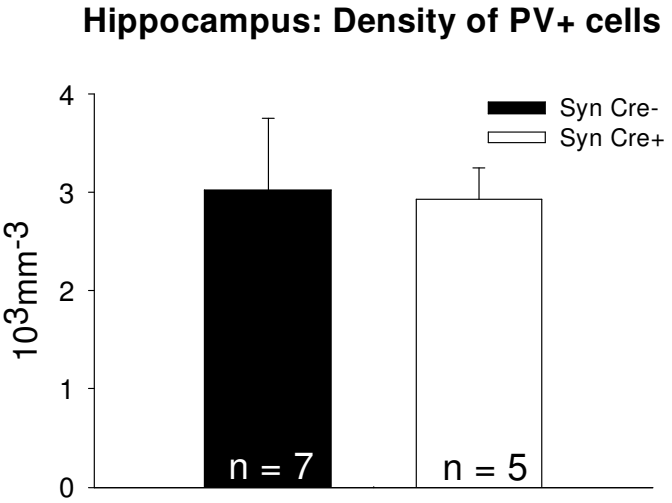

Figure 36 Density of PV+ cells in the hippocampus of Syn Cre- mice (black bar) and Syn Cre+ littermates (white bar). Numbers of animals studied per group (n) are indicated. Shown are mean values + SD. No significant difference was found (p > 0.05, t test).

4.2.3.5 **Density of Iba1-positive cells of the hippocampus**

The Iba1-postive cell density was found to be similar in conditional Syn Cre+ CHL1 deficient animals and wild type animals (Fig. 37).

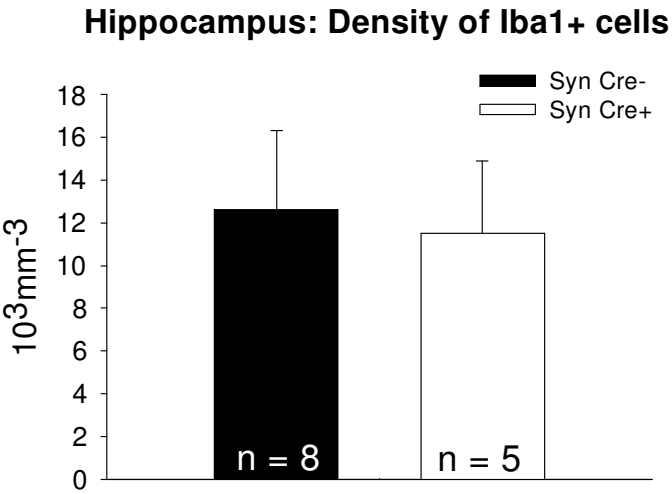

Figure 37 Density of Iba1+ cells in the hippocampus of Syn Cre- mice (black bas) and Syn Cre+ littermates (white bar). Numbers of animals studied per group (n) are indicated. Shown are mean values + SD. No significant difference was found (p > 0.05. t test).

4.2.4 **Stereological analysis of substantia nigra of Syn Cre+ mice**

4.2.4.1 **Density of TH-positive cells in substantia nigra**

The estimation of numerical densities of dopaminergic (tyrosin-hydroxylase–positive) cells revealed no significant differences between Syn Cre+ mutant and wild-type control animals (Fig. 38)

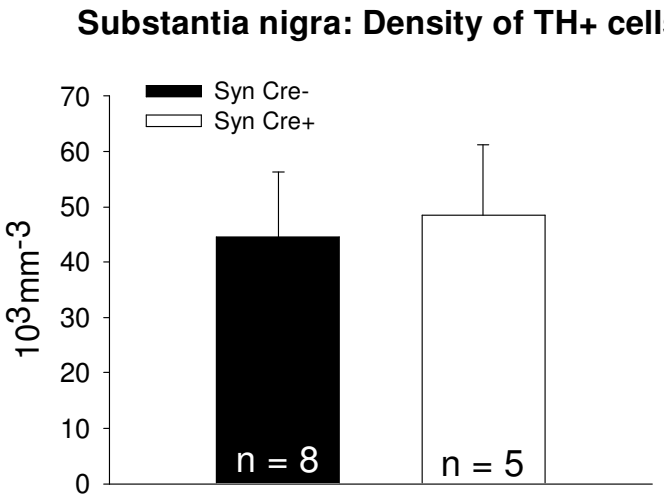

Figure 38 Density of TH+ cells in substantia nigra of Syn Cre- mice (black bar) and Syn Cre+ littermates (white bar). Numbers of animals studied per group (n) are indicated. Shown are mean values + SD. No significant difference was found ($p > 0.05$, t test).

4.2.5 **Immunohistochemical analysis of CHL1 expression of Syn Cre+ mice**

To verify that the conditional CHL1 ablation has been effective in the cortex and the hippocampus, sections from all Syn Cre+ and Syn Cre- mice analyzed morphologically were stained with a CHL1-specific antibody. The immunofluorescence staining revealed surprisingly high variability in CHL1 expression among Syn Cre+ mice. In some mutant mice CHL1 was, as expected, only weakly detectable in the hippocampus and neocortex (Fig. 40A), but in other animals the immunofluorescence signal was relatively strong (Fig. 40B). These observations suggest that the CHL1 conditional ablation was incomplete and degree of protein expression greatly varied among individual mice at the age of 12 months.

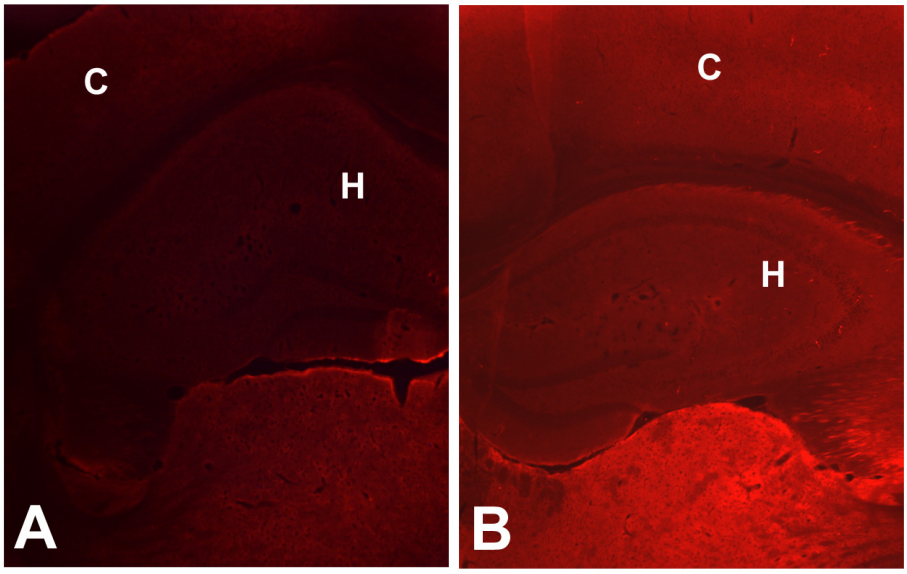

Figure 39 Immunofluorescence detection of CHL1 in coronal sections from two Syn Cre- mice. In one of these animals (A) immunostaining in the cortex (C) and the hippocampus (H) is weak. In the other Syn Cre- mouse, however, moderate intensity of the immunofluorescence is seen in the cortex and the hippocampus.

5 Discussion

5.1 Structural aberrations in the CaMKII CHL1 deficient mouse

The results of this study show that deficient expression of CHL1 in the adult mouse forebrain causes fewer abnormalities compared with constitutive CHL1 deficient mice. Apart from discrete gross structural malformations, subpopulations of inhibitory cells and dopaminergic neurons are affected in an age-dependent and brain region-specific manner in constitutive CHL1 deficient mice (Thilo, 2006). These aberrations were not observed when CHL1 was ablated in the late (postnatal) period of development using the CaMKII-driven Cre/loxP system (Table 4). While these findings are not surprising, the conditional mutation interestingly resulted in changes in the motor cortex not previously observed in constitutive CHL1 deficient mice indicating that CHL1 has age-dependent functions in specific brain regions.

Table 4. Summary of differences found between 7-month-old conditional CHL1 deficient mice (CHL1 CaMKII Cre+) and 6-month-old constitutive CHL1 deficient mice (CHL1-/-) as compared with their respective wild-type littermates in different brain regions. The time between inactivation of the CHL1 gene and time-point of analyses is similar for the two mice lines. Arrows indicate significantly lower (↓) and higher (↑) values in conditional or constitutive mutant mice as compared to littermates, = indicates no significant changes.

Gross anatomical variables	**Constitutive CHL1-/- mice (6 months)**	**CHL1 CaMKII Cre+ mice (7 months)**
Brain mass	↓	=
Volume of the lateral ventricles	↑	=
Volume of third ventricle	↑	=

Motor cortex	**Constitutive CHL1-/- mice (6 months)**	**CHL1 CaMKII Cre+ mice (7 months)**
Cortical thickness	=	↑
Total cell density	↓	=
Density of NeuN+ cells	=	↑
Density of PV+ cells	=	=
Density of reelin+ cells	↓	=
Density of Iba1+ cells	=	=

Hippocampus	**Constitutive CHL1-/- mice (6 months)**	**CHL1 CaMKII Cre+ mice (7 months)**
Volume of the hippocampus	=	=
Volume of stratum pyramidale hippocampi	↑	=
Volume of stratum granulosum area dentatae	=	=
Total cell density of stratum pyramidale in CA1	Not analyzed	=
Density of PV+ cells	↓	=
Density of Iba1+ cells	=	=

Substantia nigra	**Constitutive CHL1-/- mice (6 months)**	**CHL1 CaMKII Cre+ mice (7 months)**
Density of TH+ cells	↓	=

Amygdala	Constitutive CHL1-/- mice (6 months)	CHL1 CaMKII Cre+ mice (7 months)
Total cell density	Not analyzed	=
Density of NeuN+ cells	Not analyzed	=
Density of PV+ cells	Not analyzed	=

5.2 Structural aberrations in the Syn CHL1 deficient mouse

Since the synapsin I promoter is activated during embryonic development and is active in all neurons, in contrast to the late (postnatal) ablation of CHL1 only in excitatory neurons via the CaMKII promoter, we expected that the Syn Cre+ mouse has a more pronounced phenotype than the CaMKII mouse. With one respect this was true, similar to constitutive CHL1-/- mice, Syn Cre+ mice had much larger ventricles compared with wild-type littermates (Table 5). Surprisingly, for none of the other parameters studied did Syn Cre+ mice differ from wild-type mice (Table 5). This latter observation, in conjunction with the fact that CHL1 is normally expressed already at embryonic day 13, can be interpreted as an indication that most structural variables analyzed are influenced by CHL1 expression before the strong activation of the synapsin I promoter during late embryonic development. However, the finding that variable, often high levels of CHL1 protein were immunohistochemically detectable in the cortex and hippocampus of the analyzed Syn Cre+ mice, suggests that the lack of effects in these mice can be attributed to inefficacy of the synapsin I-mediated CHL1 ablation. Indeed, a recent R26R reporter analysis has shown that knocking out of neuronal expression in the brain, specifically in the hippocampus and neocortex, is not efficient in the Syn Cre+ mouse (Dr. Fabio Morellini, personal communication). Therefore, it can be concluded that the Syn Cre+ mouse is a doubtful model for analyses of conditional gene inactivation.

Table 5. Summary of differences found between 12-month-old conditional CHL1 deficient mice (CHL1 Syn Cre+) and 12-month-old constitutive CHL1 deficient mice (CHL1-/-) as compared with their respective wild-type littermates in different brain regions. The time between inactivation of the CHL1 gene and time-point of analyses is similar for the two mice lines. Arrows indicate significantly lower (↓) and higher (↑) values in conditional or constitutive mutant mice as compared to littermates, = indicates no significant changes.

Gross anatomical variables	**Constitutive CHL1-/- mice (12 months)**	**CHL1 Syn Cre+ mice (12 months)**
Brain mass	↑	=
Volume of lateral ventricular system	↑	↑
Volume of third ventricular system	↑	↑

Motor cortex	**Constitutive CHL1-/- mice (12 months)**	**CHL1 Syn Cre+ mice (12 months)**
Cortical thickness	=	=
Total cell density	↓	=
Density of NeuN+ cells	=	=
Density of PV+ cells	=	=
Density of reelin+ cells	↓	=
Density of Iba1+ cells	=	=

Hippocampus	Constitutive CHL1-/- mice (12 months)	CHL1 Syn Cre+ mice (12 months)
Volume of the hippocampus	=	=
Volume of stratum pyramidale hippocampi	=	=
Volume of stratum granulosum area dentatae	=	=
Density of PV+ cells	↓	=
Density of Iba1+ cells	=	=

Substantia nigra	Constitutive CHL1-/- mice (12 months)	CHL1 Syn Cre+ mice(12 months)
Density of TH+ cells	↓	=

5.3 Age-dependent and cell type-specific CHL1 expression and brain development

The major goal of this study was to dissect the role of CHL1 for brain development using conditional mutants in which the protein is ablated in a cell type-specific and age-dependent manner. The efficacy of such an approach is apparent if we consider the results on ventricular volumes. Conditional CHL1 ablation causes a large increase in the brain ventricles (Thilo, 2006). Synapsin I-mediated ablation, presumably initiated in neurons during late embryonic development, also results in ventricular enlargement. However, postnatal ablation in excitatory neurons in the forebrain using the CaMKII promoter has no effect on the ventricles. Therefore, despite doubts about the efficacy of the Syn Cre+ mediated ablation in adult mice, the combined observations indicate that CHL1 expression in neurons during embryonic development is essential for normal ventricular development. It is not clear how this CHL1 regulation

is exerted but the ventriculomegalia in the constitutive and the Syn Cre+ mouse is apparently not due to hypoplasia of major brain structures like hippocampus or neocortex, or overall brain underdevelopment.

Another important observation in this study is that postnatal ablation of CHL1 in excitatory neurons (CaMKII promoter) does not alter the structure of the hippocampus but leads, in contrast to the constitutive CHL1 ablation, to cortical hyperplasia associated with increased density of NeuN+ neurons. Since about 80% of the cortical NeuN+ neurons are excitatory (Irintchev et al., 2005), one can assume a causative relationship between the cell type-specific CHL1 ablation and increase in cortical thickness. Since CHL1 is normally expressed during the embryonic development, the time period of neuronogenesis, in the conditional mutant, the increased number of excitatory neurons in the adult can only be explained by reduced naturally occurring cell death in the postnatal period when CHL1 is already reduced in its expression. While this explanation seem plausible, it is not clear how could the absence of CHL1, a molecule known to promote cell survival, lead to decreased death of the affected neurons.

Finally, consideration requires the observation of normal numbers of microglial cells in the cortex and hippocampus of CHL1 CaMKII Cre+ mice. Estimation of microglial cell numbers is important for analyses of mutant mice since this gives the opportunity to detect pathological processes that might not be apparent using routine histology (Irintchev et al., 2005). The finding of normal numbers of $Iba1^+$ microglial cells in the conditional CHL1 mouse indicates lack of progressive neurodegeneration associated with loss of CHL1 expression in excitatory neurons.

5.3 CHL1 and psychiatric diseases

Several features of the constitutive CHL1 deficient mouse deserve attention with regard to its usefulness in neuropsychiatric research. Structural aberrations are found in these animals, as shown by previous work (Montag-Sallaz et al., 2002; Thilo, 2006), indicating the developmental significance of CHL1. These aberrations are, importantly, not severe malformations but rather discrete abnormalities as those documented in schizophrenia patients (Falkai et al., 2001; Halliday, 2001). Among the structural defects observed in the CHL1 deficient mouse are defects in connectivity of hippocampal and olfactory circuitries as suggested to occur in schizophrenia (Frankle et

al., 2003; Winterer and Weinberger, 2004). And, as shown by Thilo (2006), there are abnormal postnatal changes in distinct cell populations in the CHL1-/- mouse similar to the developmental delays in the natural history of schizophrenia and bipolar disorders. Furthermore, a sensorimotor gating deficit, assumed to be a major pathophysiological mechanism in the etiology of psychosis, is present in both heterozygous and homozygous CHL deficient mice as indicated by disrupted prepulse inhibition (Irintchev et al., 2004). Also, the behavior of the animals is different from that of normal wild-type littermates (Montag-Sallaz et al., 2002; Pratte et al., 2003), as should be expected for a model of psychosis. There are deficiencies in the structure and function of inhibitory synapses in CHL1-/- animals (Nikonenko et al., 2004) and this observation is intriguing in view of the findings that GABAergic transmission is affected in patients with psychoses (Blum and Mann, 2002; Lewis et al., 2004, Lewis et al., 1999; Reynolds et. al., 2004). And finally, there is evidence that the CHL1 gene in humans is among the susceptibility genes for schizophrenia (Lewis et al. 2003; Sakurai et al., 2002). Despite some similarities to characteristic features of human diseases, in particular psychoses, the CHL1 deficient mouse apparently does not represent the full spectrum of schizophrenic symptoms. Not only may the mouse poorly reproduce the broad spectrum of disturbances present in diseases affecting the highest cognitive and mental functions of the human brain (Marcotte et al., 2001), but if psychiatric disorders may result from “two-hits” – one genetic and the other epigenetic (Lewis and Levitt, 2002; Walker et al., 2004), the CHL-/- mouse may be considered “predisposed” rather than “diseased”: the mutant shows some functional and structural abnormalities due to the first, genetic “hit”, but a second environmental insult may be required for the development of pronounced disease symptoms.

This study shows that most of the structural aberrations described in the constitutive CHL1 deficient mouse do not occur if CHL1 is ablated after the second postnatal week (CaMKII Cre+ mice). Therefore, at first glance, surprising is the recent finding (Kolata et al., 2008) that these conditional CHL1-deficient mice have a widespread impairment of working memory duration, a finding suggesting a role for CHL1 in the short-term maintenance of information in the adult brain. Considering this functional deficit and the present observation of cortical abnormalities in the CHL1 CaMKII Cre+ mouse, it can be concluded that postnatal maintenance of CHL1 expression in excitatory neurons is essential for specific aspects of the structural organization and function of the brain.

6 Summary

The cell adhesion molecule CHL1, close homologue of L1, is associated, when mutated, with mental and psychiatric disorders in humans. Previous work has shown that constitutive CHL1 deficiency in mice causes developmental gross-anatomical abnormalities such as an age-related postnatal increase in the total brain mass and volume, enlarged brain ventricles, and hippocampal dysplasia. In addition, these mice show age-related alterations in the size of major neuronal and glial cell populations in areas typically affected in patients with schizophrenia such as the cortex and hippocampus, as well as abnormalities in nuclei providing dopaminergic innervation of the forebrain. These results raised the question at which time points of normal brain development and maturation is CHL1 of crucial importance. This question was addressed here by using two conditional CHL1-deficient mouse lines in which the CHL1 gene is ablated using the Cre/loxP technology. In one of the mouse lines analyzed here, the Cre/loxP system was driven by the synapsin I promoter (Syn line). In this mouse line CHL1 ablation was expected to be achieved during late embryogenesis and early postnatal life when synapsin I expression reaches high levels in all brain regions. In the second mouse line used, the Cre/loxP system is driven by the CaMKII promoter (CaMKII line). Under this promoter, CHL1 ablation occurs late during postnatal development, i.e. between 14 and 40 days of age, and is restricted to excitatory neurons in the forebrain. Analyses of gross anatomical variables and defined cell populations in the hippocampus, motor cortex and substantia nigra, areas known to be affected in adult mice constitutively deficient in CHL1 expression, revealed no structural aberrations, as compared with wild-type littermates, in adult (12-month-old) CHL1 deficient mice from the Syn line except for enlarged ventricles. Immunhistochemical analysis of CHL1 expression in these conditional mutants showed considerable amounts of CHL1 protein in the forebrain indicating that the conditional ablation is not efficient during adulthood. Also compared with wild-type littermates, adult (7-month-old) CaMKII CHL1 deficient mice showed no structural abnormalities except for a significant increase of the thickness of the motor cortex associated with increased number of excitatory neurons. These results suggest that the structural aberrations observed in constitutive CHL1 deficient mice arise during early development of the brain. In addition, the finding of cortical hyperplasia in the CaMKII

CHL1 deficient mice and the recent finding of impaired working memory duration in these mice suggest that normal levels of postnatal CHL1 expression in excitatory forebrain neurons are essential for specific aspects of the structural organization and function of the brain.

7 References

AbdelMalik P, Husted J, Chow EW, Bassett AS. (2003) Childhood head injury and expression of schizophrenia in multiply affected families.
Arch Gen Psychiatry. 60: 231-6.

Akbarian S, Kim JJ, Potkin SG, Hagman JO, Tafazzoli A, Bunney WE Jr, Jones EG. (1995) Gene expression for glutamic acid decarboxylase is reduced without loss of neurons in prefrontal cortex of schizophrenics.
Arch Gen Psychiatry 52: 258-66.

Andersen SL (2003) Trajectories of brain development: point of vulnerability or window of opportunity?
Neurosci Biobehav Rev. 27: 3-18.

Angeloni D, Lindor NM, Pack S, Latif F, Wei MH, Lerman MI.(1999) CALL gene is haploinsufficient in a 3p- syndrome patient.
Am J Med Genet. 86: 482-5.

Angevine JB Jr, Sidman RL. (1961) Autoradiographic study of cell migration during histogenesis of cerebral cortex in the mouse.
Nature.192: 766-8.

Arnold SE, Gur RE, Shapiro RM, Fisher KR, Moberg PJ, Gibney MR, Gur RC, Blackwell P, Trojanowski JQ.(1995) Prospective clinicopathologic studies of schizophrenia: accrual and assessment of patients.
Am J Psychiatry. 152: 731-7.

Asai M, Ito Y, Iguchi T, Ito J, Okada N, Oishi H.(1992) Terminal deletion of the short arm of chromosome 3.
Jpn J Hum Genet. 37: 163-8.

Atashi JR, Klinz SG, Ingraham CA, Matten WT, Schachner M, Maness PF (1992) Neural cell adhesion molecules modulate tyrosine phosphorylation of tubulin in nerve growth cone membranes.
Neuron.8: 831-42.

Austin CP, Ky B, Ma L, Morris JA, Shughrue PJ (2004) Expression of Disrupted-In-Schizophrenia-1, a schizophrenia-associated gene, is prominent in the mouse hippocampus throughout brain development.
Neuroscience. 24: 3-10.

Barr CE, Mednick SA, Munk-Jorgensen P (1990) Exposure to influenza epidemics during gestation and adult schizophrenia. A 40-year study.
Arch Gen Psychiatry. 47: 869-74.

Bayer KU, Löhler J, Schulman H, Harbers K (1999) Developmental expression of the CaM kinase II isoforms: ubiquitous gamma- and delta-CaM kinase II are

the early isoforms and most abundant in the developing nervous system.
Brain Res Mol Brain Res. 70: 147-54.

Benes FM, Davidson J, Bird ED (1986) Quantitative cytoarchitectural studies of the cerebral cortex of schizophrenics..
Arch Gen Psychiatry. 43: 31-5.

Benes FM, Kwok EW, Vincent SL, Todtenkopf MS. (1998) A reduction of nonpyramidal cells in sector CA2 of schizophrenics and manic depressives.
Biol Psychiatry. 5;44: 88-97.

Benes FM, McSparren J, Bird ED, SanGiovanni JP, Vincent SL (1991) Deficits in small interneurons in prefrontal and cingulate cortices of schizophrenic and schizoaffective patients.
Arch Gen Psychiatry. 48: 996-1001

Benes FM, Sorensen I, Bird ED (1991) Reduced neuronal size in posterior hippocampus of schizophrenic patients.
Schizophr Bull.17: 597-608.

Bixby JL, Lilien J, Reichardt LF (1988) Identification of the major proteins that promote neuronal process outgrowth on Schwann cells in vitro.Bixby JL, Lilien J, Reichardt LF.
J Cell Biol. 107: 353-61.

Blum BP, Mann JJ (2002) The GABAergic system in schizophrenia.
Int J Neuropsychopharmacol 5:159-179

Brown AS, Cohen P, Harkavy-Friedman J, Babulas V, Malaspina D, Gorman JM, Susser ES.(2001) Bennett A.E (1970) Research Award. Prenatal rubella, premorbid abnormalities, and adult schizophrenia.
Biol Psychiatry. 49: 473-86.

Brümmendorf T, Rathjen FG (1993) Axonal glycoproteins with immunoglobulin- and fibronectin type III-related domains in vertebrates: structural features, binding activities, and signal transduction.
J Neurochem. 61: 1207-19. Review.

Brümmendorf T, Rathjen FG (1994) Cell adhesion molecules. 1: immunoglobulin superfamily.
Protein Profile. 1: 951-1058. Review.

Brümmendorf T, Rathjen FG (1995) Cell adhesion molecules 1: immunoglobulin superfamily.
Protein Profile. 2: 963-1108.

Buhusi M, Midkiff BR, Gates AM, Richter M, Schachner M, Maness PF (2003) Close homolog of L1 is an enhancer of integrin-mediated cell migration.
J Biol Chem. 278: 25024-31.

Bukalo O, Fentrop N, Lee AY, Salmen B, Law JW, Wotjak CT, Schweizer M, Dityatev A, Schachner M (2004) Conditional ablation of the neural cell

adhesion molecule reduces precision of spatial learning, long-term potentiation, and depression in the CA1 subfield of mouse hippocampus.
J Neurosci. 24: 1565-77.

Cancro R.(1989) The art of turf creation.
Arch Gen Psychiatry. 46: 191-4.

Cannon M, Murray RM.(1998) Neonatal origins of schizophrenia.
Arch Dis Child. 78: 1-3

Cannon TD, Rosso IM, Hollister JM, Bearden CE, Sanchez LE, Hadley T.(2000) A prospective cohort study of genetic and perinatal influences in the etiology of schizophrenia.
Schizophr Bull. 26: 351-66.

Carola A, Haas and Louis J. DeGennaro (1988) Multiple Synapsin I messager rnas are differentially regulated during neuronal development.
The J of Cell Biol.106: 195-203

Chaisuksunt V, Zhang Y, Anderson PN, Campbell G, Vaudano E, Schachner M, Lieberman AR (2000) Axonal regeneration from CNS neurons in the cerebellum and brainstem of adult rats; correlation with the patterns of expression and distribution of messenger RNAs for L1, CHL1, c-jun and growth-associated protein-43.
Neuroscience 100: 87-108.

Chen QY, Chen Q, Feng GY, Lindpaintner K, Chen Y, Sun X, Chen Z, Gao Z, Tang J, He L (2005) Case-control association study of the close homologue of L1 (CHL1) gene and schizophrenia in the Chinese population.
Schizophr Res. 73: 269-74.

Chen S, Mantel L, Dong L, Schachner M (1999) Prevention of neuronal cell death by neural adhesion molecules L1 and CHL1.
J Neurobiol 38: 428-439

Cohen NR, Taylor JSH, Scott LB, Guillery RW, Soriano P, Furley AJW (1997) Errors in corticospinal axon guidance in mice lacking the neural cell adhesion molecule L1.
Curr Biol 7: 26-33.

Collinson JM, Marshall D, Gillespie CS, Brophy PJ (1998) Transient expression of neurofascin by oligodendrocytes at the onset of myelinogenesis: implications for mechanisms of axon-glial interaction.
Glia.23: 11-23.

Costa E, Chen Y, Davis J, Dong E, Noh J.S, Tremolizzo L, Veldic M, Grayson D.R, Guidotti A (1998) A decrease of reelin expression as a putative vulnerability factor in schizophrenia
Proc Natl Acad Sci USA 95: 15718-23.

Cunningham BA (1995) Cell adhesion molecules as morphoregulators.
Curr Opin Cell Biol.7: 628-33.

Dahme M, Bartsch U, Martini R, Anliker B, Schachner M, Mantei N (1997) Disruption of the mouse L1 gene leads to malformations of the nervous system.
Nat Genet. 17: 346-9.

DeBernardo, AP; Chang, S. (1996) Heterophilic interactions of DM-GRASP: GRASP-NgCAM interactions involved in neurite extension.
J Cell Biol.133: 657–666

De Camilli P, Harris SM Jr, Huttner WB, Greengard P (1983) Synapsin I (Protein I), a nerve terminal-specific phosphoprotein. II. Its specific association with synaptic vesicles demonstrated by immunocytochemistry in agarose-embedded synaptosomes.
J Cell Biol. 96: 1355-73.

Demyanenko GP, Schachner M, Anton E, Schmid R, Feng G, Sanes J, Maness PF (2004) Close homolog of L1 modulates area-specific neuronal positioning and dendrite orientation in the cerebral cortex.
Neuron. 2004 44: 423-37.

Dennert JW, Andreasen NC.(1983) Ct scanning and schizophrenia: a review
Psychiatr Dev. Spring; 1: 105-22

Edelmann CM Jr (1970) The genetics of primary renal tubular acidosis.
Birth Defects Orig Artic Ser.6: 25-6.

Falkai P, Bogerts B. (1986) Cell loss in the hippocampus of schizophrenics.
Eur Arch Psychiatry Neurol Sci. 236: 154-61.

Falkai P, Bogerts B, Rozumek M. (1988) Limbic pathology in schizophrenia: the entorhinal region--a morphometric study.
Biol Psychiatry. 24: 515-21

Falkai P, Vogeley K, Maier W (2001) Hirnstrukturelle Veränderungen bei Patienten mit schizophrenen Psychosen.
Nervenarzt 72:331-341

Feinberg I (1982-1983) Schizophrenia: caused by a fault in programmed synaptic elimination during adolescence?
J Psychiatr Res.17; 319-34.

Flaum M, Arndt S, Andreasen NC (1990) The role of gender in studies of ventricle enlargement in schizophrenia: a predominantly male effect.
Am J Psychiatry. 147: 1327-32.

Florin L, Alter H, Gröne HJ, Szabowski A, Schütz G, Angel P (2004) Cre recombinase-mediated gene targeting of mesenchymal cells.
Genesis 38: 139-44.

Frankle WG, Lerma J, Laurelle M (2003) The synaptic hypothesis of schizophrenia.
Neuron 39:205-216

Franklin KBJ, Paxinos G (1997) The mouse brain in stereotaxic coordinates. Academic.Press, San Diego

Fransen E, D'Hooge R, Van Camp G, Verhoye M, Sijbers J, Reyniers E, Soriano P, Kamiguchi H, Willemsen R, Koekkoek SK, De Zeeuw CI, De Deyn PP, Van der Linden A, Lemmon V, Kooy RF, Willems PJ. (1998) L1 knockout mice show dilated ventricles, vermis hypoplasia and impaired exploration patterns. Hum Mol Genet. 7: 999-1009.

Frints SG, Marynen P, Hartmann D, Fryns JP, Steyaert J, Schachner M, Rolf B, Craessaerts K, Snellinx A, Hollanders K, D'Hooge R, De Deyn PP, Froyen G (2003) CALL interrupted in a patient with non-specific mental retardation: gene dosage-dependent alteration of murine brain development and behavior. Hum Mol Genet.12: 1463-1474.

Gerber DJ, Hall D, Miyakawa T, Demars S, Gogos JA, Karayiorgou M, Tonegawa S (2003) Evidence for association of schizophrenia with genetic variation in the 8p21.3 gene, PPP3CC, encoding the calcineurin gamma subunit. Proc Natl Acad Sci U S A. 100: 8993-8.

Goodman CS, Shatz CJ (1993), Developmental mechanisms that generate precise patterns of neuronal connectivity. Cell 72:77-98

Gottesmann I.I (1991) Schizophrenia Genesis: The Origins of Madness. W. H. Freeman, New York.; Review (1993) Behavior genetics 23: 01-8244

Gottesman and Shields (1976) A Critical Review of Recent Adoption, Twin, and Family Studies of Schizophrenia: Behavioral Genetics Perspectives Schizophr Bull 2: 360-401;

Green MF, Kern RS, Braff DL, Mintz J (2000) Neurocognitive deficits and functional outcome in schizophrenia: are we measuring the "right stuff"? Schizophr Bull. 26: 119-36.

Haas CA, DeGennaro LJ (1988) Multiple synapsin I messenger RNAs are differentially regulated during neuronal development. J Cell Biol. 106: 195-203.

Halliday GM (2001) A review of the neuropathology of schizophrenia. Clin Exp Pharmacol Physiol 28:64-65

Harrison PJ (1999) The neuropathology of schizophrenia. A critical review of the data and their interpretation. Brain. 122: 593-624.

Harrison PJ, Weinberger DR (2005) Schizophrenia genes, gene expression, and neuropathology: on the matter of their convergence. Mol Psychiatry. 10: 40-68; Erratum in: Mol Psychiatry. 2005 10: 420. Mol Psychiatry. 2005 10: 804.

Heckers S, Heinsen H, Geiger B, Beckmann H. (1991) Hippocampal neuron number in schizophrenia. A stereological study.
Arch Gen Psychiatry. 48: 1002-1008.

Hillenbrand R, Molthagen M, Montag D, Schachner M (1999) The close homologue of the neural adhesion molecule L1 (CHL1): patterns of expression and promotion of neurite outgrowth by heterophilic interactions.
Eur J Neurosci. 11: 813-826.

Hlavin ML, Lemmon V (1991) Molecular structure and functional testing of human L1CAM: an interspecies comparison.
Genomics. 11: 416-423.

Holm J, Hillenbrand R, Steuber V, Bartsch U, Moos M, Lübbert H, Montag D, Schachner M (1996) Structural features of a close homologue of L1 (CHL1) in the mouse: a new member of the L1 family of neural recognition molecules.
Eur J Neurosci. 8: 1613-1629.

Howard CV and Reed MG (1998) Surface-weighted star volume: concept and estimation.
J Microsc. 190: 350-6.

Ignelzi MA Jr, Miller DR, Soriano P, Maness PF (1994) Impaired neurite outgrowth of src-minus cerebellar neurons on the cell adhesion molecule L1.
Neuron. 12: 873-884.

Imai Y, Kohsaka S (2002) Intracellular signaling in M-CSF-induced microglia activation: role of Iba1.
Glia. 40: 164-174.

Irintchev A, Koch M, Needham LK, Maness P, Schachner M (2004) Impairment of sensorimotor gating in mice deficient in the cell adhesion molecule L1 or its close homologue, CHL1.
Brain Res. 1029: 131-134.

Irintchev A, Rollenhagen A, Troncoso E, Kiss JZ, Schachner M (2005) Structural and functional aberrations in the cerebral cortex of tenascin-C deficient mice.
Cereb Cortex 15: 950-962

Jakob H, Beckmann H (1986).Prenatal developmental disturbances in the limbic allocortex in schizophrenics.
J Neural Transm. 65: 303-26.

Jeste DV, Lohr JB.(1989) Hippocampal pathologic findings in schizophrenia. A morphometric study.
Arch Gen Psychiatry. 46: 1019-24

Jiao Y, Sun Z, Lee T, Fusco FR, Kimble TD, Meade CA, Cuthbertson S, Reiner A (1999) A simple and sensitive antigen retrieval method for free-floating and slide-mounted tissue sections.
J Neurosci Methods. 93: 149-162.

Kamiguchi H, Lemmon V (1997) Neural cell adhesion molecule L1: signaling pathways and growth cone motility.
J Neurosci Res. 49: 1-8.

Kaplan P (1983) X linked recessive inheritance of agenesis of thge corpus callosum.
J.Med.Genet. 20: 122-124.

Keith SJ, Matthews SM (1991) The diagnosis of schizophrenia: a review of onset and duration issues.
Schizophr Bull. 17: 51-67.

Kenwrick, Watkins, De Angelis (2000) Neural cell recognition molecule L1: relating biological complexity to human disease mutations
Human Molecular Genetics 6: 879-886

Kindermann SS, Karimi A, Symonds L, Brown GG, Jeste DV (1997) Review of functional magnetic resonance imaging in schizophrenia.
Schizophr Res. 27: 143-56.

Klinz SG, Schachner M, Maness PF (1995) L1 and N-CAM antibodies trigger protein phosphatase activity in growth cone-enriched membranes.
J Neurochem. 65: 84-95.

Kolata S, Wu J, Light K, Schachner M, Matzel LD (2008) Impaired working memory duration but normal learning abilities found in mice that are conditionally deficient in the close homolog of L1.
J Neurosci 28: 13505-13510.

Kulhara P, Chakrabarti S (2001) Culture and schizophrenia and other psychotic disorders.
Psychiatr Clin North Am. 24: 449-64.

Kurumaji A, Nomoto H, Okano T, Toru M (2001) An association study between polymorphism of L1CAM gene and schizophrenia in a Japanese sample.
Am J Med Genet. 105: 99-104.

Lagenaur C, Lemmon V (1987) An L1-like molecule, the 8D9 antigen, is a potent substrate for neurite extension.
Proc Natl Acad Sci U S A.84: 7753-7.

Lauriello J, Hoff A, Wieneke MH, Blankfeld H, Faustman WO, Rosenbloom M, DeMent S, Sullivan EV, Lim KO, Pfefferbaum A (1997) Similar extent of brain dysmorphology in severely ill women and men with schizophrenia.
Am J Psychiatry.154: 819-25.

Law JW, Lee AY, Sun M, Nikonenko AG, Chung SK, Dityatev A, Schachner M, Morellini F (2003) Decreased anxiety, altered place learning, and increased CA1 basal excitatory synaptic transmission in mice with conditional ablation of the neural cell adhesion molecule L1.
J Neurosci. 23: 10419-32.

Lawrie SM, Abukmeil SS (1998) Brain abnormality in schizophrenia. A systematic and quantitative review of volumetric magnetic resonance imaging studies Br J Psychiatry. 172: 110-20.

Lemmon, Farr, Lagenaur (1989) L1-mediated axon outgrowth occurs via a homophilic binding mechanism.
Neuron. 2:1597-603

Leshchyns'ka I, Sytnyk V, Richter M, Andreyeva A, Puchkov D, Schachner (2006) The adhesion molecule CHL1 regulates uncoating of clathrin-coated synaptic vesicles.
M.Neuron. 52: 1011-25.

Lewis CM, Levinson DF, Wise LH, DeLisi LE, Straub RE, Hovatta I et al. (2003) Genome Scan Meta-Analysis of Schizophrenia and Bipolar Disorder, Part II: Schizophrenia.
Am J Hum Genet 73:34-48

Lewis DA, Levitt P (2002) Schizophrenia as a disorder of neurodevelopment.
Annu Rev Neurosci 25:409-432

Lewis DA, Pierri JN, Volk DW, Melchitzky DS, Woo TU (1999) Altered GABA neurotransmission and prefrontal cortical dysfunction in schizophrenia.
Biol Psychiatry. 46: 616-26.

Lewis DA, Volk DW, Hashimoto T (2004) Selective alterations in prefrontal cortical GABA neurotransmission in schizophrenia: a novel target for the treatment of working memory dysfunction. Psychopharmacology (Berl) 174:143-150

Liu Q, Dwyer ND, O'Leary DD (2000) Differential expression of COUP-TFI, CHL1, and two novel genes in developing neocortex identified by differential display PCR.
J Neurosci. 20: 7682-90.

Lu B, Greengard P, Poo MM (1992) Exogenous synapsin I promotes functional maturation of developing neuromuscular synapses.
Neuron. 8: 521-9.

Lu P, Jones LL, Tuszynski MH (2007) Axon regeneration through scars and into sites of chronic spinal cord injury.
Exp Neurol. 203: 8-21.

Lüthl A, Laurent JP, Figurov A, Muller D, Schachner M (1994) Hippocampal long-term potentiation and neural cell adhesion molecules L1 and NCAM
Nature. 372: 777-9.

Ma L, Liu Y, Ky B, Shughrue PJ, Austin CP, Morris JA (2002) Cloning and characterization of Disc1, the mouse ortholog of DISC1 (Disrupted-in-Schizophrenia 1).
Genomics.80: 662-72.

Mantamadiotis T, Lemberger T, Bleckmann SC, Kern H, Kretz O, Martin Villalba A, Tronche F, Kellendonk C, Gau D, Kapfhammer J, Otto C, Schmid W, Schütz G (2002) Disruption of CREB function in brain leads to neurodegeneration.
Nat Genet. 31: 47-54.

Marcotte ER, Pearson DM, Srivastava LK (2001) Animal models of schizophrenia: a critical review.
J Psychiatry Neurosci 26:395-410

Mason MR, Lieberman AR, Anderson PN (2003) Corticospinal neurons up-regulate a range of growth-associated genes following intracortical, but not spinal, axotomy.
Eur J Neurosci 18: 789-802.

Mayford M, Wang J, Kandel ER, O'Dell TJ (1995) CaMKII regulates the frequency-response function of hippocampal synapses for the production of both LTD and LTP.
Cell. 81: 891-904.

Melloni RH Jr, DeGennaro LJ (1994) Temporal onset of synapsin I gene expression coincides with neuronal differentiation during the development of the nervous system.
J Comp Neurol. 342: 449-462.

Montag-Sallaz M, Schachner M, Montag D (2002) Misguided axonal projections, neural cell adhesion molecule 180 mRNA upregulation, and altered behavior in mice deficient for the close homolog of L1.
Mol Cell Biol. 22: 7967-7981.

Moos M, Tacke R, Scherer H, Teplow D, Früh K, Schachner M (1988) Neural adhesion molecule L1 as a member of the immunoglobulin superfamily with binding domains similar to fibronectin.
Nature. 334: 701-703.

Morellini F, Lepsveridze E, Kähler B, Dityatev A, Schachner M (2007) Reduced reactivity to novelty, impaired social behavior, and enhanced basal synaptic excitatory activity in perforant path projections to the dentate gyrus in young adult mice deficient in the neural cell adhesion molecule CHL1.
Mol Cell Neurosci. 34: 121-136.

Morris JA, Kandpal G, Ma L, Austin CP (2003) DISC1 (Disrupted-In-Schizophrenia 1) is a centrosome-associated protein that interacts with MAP1A, MIPT3, ATF4/5 and NUDEL: regulation and loss of interaction with mutation.
Hum Mol Genet. 12: 1591-1608.

Murray RM, Jones P, O'Callaghan E, Takei N, Sham P (1992) Genes, viruses and neurodevelopmental schizophrenia.
J Psychiatr Res. 26: 225-235.

Navone F, Greengard P, De Camilli P (1984) Synapsin I in nerve terminals: selective association with small synaptic vesicles.
Science. 226: 1209-1211.

Nestler EJ, Walaas SI, Greengard P (1984) Neuronal phosphoproteins: physiological and clinical implications.
Science. 225: 1357-1364.

Nikonenko AG, Sun M, Irintchev A, Dityatev A, Schachner M (2004) Physiological and structural correlates of increased perisomatic inhibition in juvenile mice deficient in the neural cell adhesion molecule CHL1.
Mol Cell Neurosci (In press)

Nikonenko AG, Sun M, Lepsveridze E, Apostolova I, Petrova I, Irintchev A, Dityatev A, Schachner M (2006) Enhanced perisomatic inhibition and impaired long-term potentiation in the CA1 region of juvenile CHL1-deficient mice.
Eur J Neurosci. 23: 1839-1852.

Nopoulos P, Flaum M, Andreasen NC (1997) Sex differences in brain morphology in schizophrenia.
Am J Psychiatry. 154: 1648-1654.

Novak A, Guo C, Yang W, Nagy A, Lobe CG (2000) Z/EG, a double reporter mouse line that expresses enhanced green fluorescent protein upon Cre-mediated excision.
Genesis. 28: 147-155

O'Rourke DH, Gottesman II, Suarez BK, Rice J, Reich T. (1982) Refutation of the general single-locus model for the etiology of schizophrenia.
Am J Hum Genet. 34: 630-649.

Pakkenberg B. (1990) Pronounced reduction of total neuron number in mediodorsal thalamic nucleus and nucleus accumbens in schizophrenics.
Arch Gen Psychiatry. 47: 1023-1028.

Panicker AK, Buhusi M, Thelen K, Maness PF (2003) Cellular signalling mechanisms of neural cell adhesion molecules.
Front Biosci 8: 900-911

Pantelis C, Velakoulis D, McGorry PD, Wood SJ, Suckling J, Phillips LJ, Yung AR, Bullmore ET, Brewer W, Soulsby B, Desmond P, McGuire PK (2003) Neuroanatomical abnormalities before and after onset of psychosis: a cross-sectional and longitudinal MRI comparison.
Lancet. 361: 281-288.

Pearlson GD (1997) Superior temporal gyrus and planum temporale in schizophrenia: a selective review. Prog Neuropsychopharmacol
Biol Psychiatry. 21: 1203-1229.

Perry W, Feifel D, Minassian A, Bhattacharjie I, Braff DL (2002) Information processing deficits in acutely psychotic schizophrenia patients medicated and

unmedicated at the time of admission.
Am J Psychiatry. 159: 1375-81.

Pesold C, Liu WS, Guidotti A, Costa E, Caruncho HJ (1999) Cortical bitufted, horizontal, and Martinotti cells preferentially express and secrete reelin into perineuronal nets, nonsynaptically modulating gene expression.
Proc Natl Acad Sci U S A. 96: 3217-3222.

Pinaudeau-Nasarre C, Gaillard A, Roger M (2002) Timing and plasticity of specification of CaM-Kinase II alpha expression by neocortical neurons.
Brain Res Dev Brain Res. 138: 97-107

Poltyrev T, Keshet GI, Kay G, Weinstock M.(1996) Role of experimental conditions in determining differences in exploratory behavior of prenatally stressed rats.
Dev Psychobiol. 29: 453-62.

Pratte M, Rougon G, Schachner M, Jamon M (2003) Mice deficient for the close homologue of the neural adhesion cell L1 (CHL1) display alterations in emotional reactivity and motor coordination.
Behav Brain Res. 147: 31-39

Rader C, Kunz B, Lierheimer R, Giger RJ, Berger P, Tittmann P, Gross H, Sonderegger P (1996) Implications for the domain arrangement of axonin-1 derived from the mapping of its NgCAM binding site.
EMBO J.15: 2056-2068.

Reichert H, Boyan G (1997) Building a brain: developmental insights in insects.
Trends Neurosci.20: 258-264.

Rempe D, Vangeison G, Hamilton J, Li Y, Jepson M, Federoff HJ (2006) Synapsin I Cre transgene expression in male mice produces germline recombination in progeny.
Genesis. 44: 44-49.

Reynolds GP, Abdul-Monim Z, Neill JC, Zhang ZJ (2004) Calcium binding protein markers of GABA deficits in schizophrenia-postmortem studies and animal models.
Neurotox Res 6:57-61

Roberts GW, Colter N, Lofthouse R, Johnstone EC, Crow TJ. (1987) Is there gliosis in schizophrenia? Investigation of the temporal lobe.
Biol Psychiatry. 22::1459-1468.

Saffell JL, Williams EJ, Mason IJ, Walsh FS, Doherty P (1997) Expression of a dominant negative FGF receptor inhibits axonal growth and FGF receptor phosphorylation stimulated by CAMs.
Neuron. 18: 231-42. Erratum in: Neuron 1998 20: 619.

Sakurai K, Migita O, Toru M, Arinami T (2002) An association between a missense polymorphism in the close homologue of L1 (CHL1, CALL) gene and schizophrenia.
Mol Psychiatry. 7: 412-415.

Sauer B (1998) Inducible gene targeting in mice using the Cre/lox system. Methods 14: 381-92.

Schachner M (1991) Cell surface recognition and neuron-glia interactions. Ann N Y Acad Sci. 633: 105-12.

Schachner M (1997) Neural recognition molecules and synaptic plasticity. Curr Opin Cell Biol 9: 627-34.

Schmajuk NA (2001) Hippocampal dysfunction in schizophrenia. Hippocampus. 11: 599-613.

Scholey AB, Rose SP, Zamani MR, Bock E, Schachner M (1993) A role for the neural cell adhesion molecule in a late, consolidating phase of glycoprotein synthesis six hours following passive avoidance training of the young chick. Neuroscience. 55: 499-509.

Schrander-Stumpel C, Fryns J, Cassiman JJ, Legius E, Spaepen A, Höweler CJ (1992) MASA syndrome (a form of complicated spastic paraplegia) and X linked hydrocephalus: variable expression of the same mutation at Xq28? Call for families.
J Med Genet. 29: 215.

Schuch U, Lohse MJ, Schachner M (1989) Neural cell adhesion molecules influence second messenger systems.
Neuron.3; 13-20.

Schwartz RC, Cohen BN (2001)Psychosocial correlates of suicidal intent among patients with schizophrenia.
Compr Psychiatry. 42: 118-23.

Schwartz RC, Smith SD. (2004) Suicidality and psychosis: the predictive potential of symptomatology and insight into illness.
J Psychiatr Res. 38: 185-91.

Shaw SH, Kelly M, Smith AB, Shields G, Hopkins PJ, Loftus J, Laval SH, Vita A, Dehert M, Cardon LR, Crow T, Sherrington R, Delisi LE. A Genome-wide search for Schizophrenia (1998) Susceptibility Genes.
American Journal of Medical Genetics 81: 364-376.

Sidman RL, Agevine JB and Peirce ET (1971) Atlas of the mouse brain and spinal cord.
Harvard University Press, Cambridge, Massachusetts

Smythe JW, Rowe WB, Meaney MJ (1994) Neonatal handling alters serotonin (5-HT) turnover and 5-HT2 receptor binding in selected brain regions: relationship to the handling effect on glucocorticoid receptor expression. Brain Res Dev Brain Res. 80: 183-9.

Solà C, Tusell JM, Serratosa J (1999) Comparative study of the distribution of calmodulin kinase II and calcineurin in the mouse brain.
J Neurosci Res. 57: 651-62.

Stoeckli ET, Ziegler U, Bleiker AJ, Groscurth P, Sonderegger P (1996) Clustering and functional cooperation of Ng-CAM and axonin-1 in the substratum-contact area of growth cones.
Dev Biol. 177: 15-29.

Street KA, Xu G, Hall KL, Intano GW, McCarrey JR, Herbert DC, Kilimann MW, Walter CA (2005) Rat synapsin 1 promoter mediated transgene expression in testicular cell types.
DNA Cell Biol. 24: 133-40

Takeda Y, Asou H, Murakami Y, Miura M, Kobayashi M, Uyemura K (1996) A nonneuronal isoform of cell adhesion molecule L1: tissue-specific expression and functional analysis.
J Neurochem. 66: 2338-49.

Thiery J. P. (2003) Cell adhesion in development: a complex signaling network.
Current Opinion in Genetics & Development 13: 365-371

Thilo B (2006) Age dependent and region-specific alterations in the brain of CHL1 deficient mice: an emerging animal-based model of schizophrenia.
Inaugural Dissertation, University of Hamburg.

Tissir F, Goffinet AM (2003) Reelin and brain development.
Nat Rev Neurosci. 4: 496-505.

Torrey EF (1987) Prevalence studies in schizophrenia.
Br J Psychiatry. 150: 598-608.

Ueda T, Greengard P (1977) Adenosine 3':5'-monophosphate-regulated phosphoprotein system of neuronal membranes. I. Solubilization, purification, and some properties of an endogenous phosphoprotein.
J Biol Chem. 252: 5155-63.

Van Camp G, Fransen E, Vits L, Raes G, Willems PJ (1996) A locus-specific mutation database for the neural cell adhesion molecule L1CAM (Xq28).
Hum Mutat. 8: 391.

Walker EF (1994) Developmentally moderated expressions of the neuropathology underlying schizophrenia.
Schizophr Bull. 20: 453-480.

Walker E, Kestler L, Bollini A, Hochman KM (2004) Schizophrenia: etiology and course.
Annu Rev Psychol. 55: 401-430.

Walker J, Curtis V, Murray RM (2002) Schizophrenia and bipolar disorder: similarities in pathogenic mechanisms but differences in neurodevelopment.
Int Clin Psychopharmacol 17 Suppl 3:S11-S19

Wei M H, Karavanova I, Ivanov S.V. Popescu N.C, Keck C.L, Pack S, Eisen J.A, Lerman M.L (1998) In silico-initiated cloning and molecular characterization of a novel human member of the L1 gene family of neural cell adhesion

molecules.Hum.
Genet. 103: 355-364.

Weinberger DR (1987) Implications of normal brain development for the pathogenesis of schizophrenia.
Arch Gen Psychiatry 44: 660-666

Welberg LA, Seckl JR (2001) Prenatal stress, glucocorticoids and the programming of the brain.
J Neuroendocrinol. 13: 113-128.

Wilson GN, Pooley J, Parker J.J (1982) The phenotype of ring chromosome 3.
Med Genet.19: 471-473.

Winterer G, Weinberger DR (2004) Genes, dopamine and cortical signal-to-noise ratio in schizophrenia.
Trends Neurosci 27:683-690

Wolf HK, Buslei R, Schmidt-Kastner R, Schmidt-Kastner PK, Pietsch T, Wiestler OD, Blümcke I (1996) NeuN: a useful neuronal marker for diagnostic histopathology.
J Histochem Cytochem. 44: 1167-1171.

Yamasaki M, Arita N, Hiraga S, Izumoto S, Morimoto K, Nakatani S, Fujitani K, Sato N, Hayakawa T (1995) A clinical and neuroradiological study of X-linked hydrocephalus in Japan.
J Neurosurg. 83: 50-55.

Yang-Feng TL, DeGennaro LJ, Francke U (1986) Genes for synapsin I, a neuronal phosphoprotein, map to conserved regions of human and murine X chromosomes.
Proc Natl Acad Sci U S A 83: 8679-8683.

Zhao X, Siu CH (1995) Colocalization of the homophilic binding site and the neuritogenic activity of the cell adhesion molecule L1 to its second Ig-like domain.
J Biol Chem. 270: 29413-29421.

Zhao X, Siu CH (1996) Differential effects of two hydrocephalus/MASA syndrome-related mutations on the homophilic binding and neuritogenic activities of the cell adhesion molecule L1.
J Biol Chem. 271: 6563-6566.

Zhu Y, Romero MI, Ghosh P, Ye Z, Charnay P, Rushing EJ, Marth JD, Parada LF (2001) Ablation of NF1 function in neurons induces abnormal development of cerebral cortex and reactive gliosis in the brain.
Genes Dev. 15: 859-876.

8 Abbreviations

A	Area
C	Cortex
CA1-CA3	Cornu ammon, region of hippocampus
Ca^{2+}	Calcium
$CaCl^2$	Calcium chloride
CaMKII	Calcium/calmodulin-dependent protein kinase II
CALL	Cell adhesion L1-like
cAMP	cyclisches Adenosinmonophosphat
CAMs	Cell adhesion molecules
CHL1	Close homologue of L1
CHL1+/+	CHL1 non deficient
CHL1-/-	CHL1 deficient
CJMs	Cell-joining molecules
Cm	centimetres
CNS	Central nervous system
Cre	Cyclization recombination
DISC1	Disrupted-in-Schizophrenia 1
DNA	desoxyribonucleinacid
E	Embryonic day
e.g.	example given
est.	estimated
FN	Fibronectin
G	gram
GABA	Gamma amino butyric acid
H	hippocampus
HSAS	Hydrocephalus due to stenosis of the aqueduct of Sylvius
i.e.	id est
Ig	Immunoglobulin
IQ	intelligence quotient
kDa	Kilodalton
Leu	Leucin

LTP	Long term potentiation
loxP	Locus of X-over P1
M	motor areas
MASA	Mental retardation, aphasia, shuffling gait, adducted thumbs
ml	Mililiter
mm	Milimeter
mM	Milimol
mRNA	Messenger ribonucleinacid
N	Number
NCAM	Neural cell adhesion molecule
NeuN	Neuron-speficic nuclear antigen
NgCAM	Neuron-glial Cell Adhesion Molecule
NrCAM	NgCAM related Cell Adhesion Molecule
PBS	Phosphate buffered saline
pH	(p)otential of (H)ydrogen,the logarithm of the reciprocal of hydrogen-ion concentration in gram pro litre
Phe	Phenylalanin
PPI	Prepulse inhibition
PV	Parvalbumin
RGS4	Regulator of G-protein signaling 4
RNA	Ribonucleinacid
RT	room temperature
S	sensory areas
SAMs	Substrate adhesion molecules
SD	Standard deviation
Syn	SynapsinI
TH	Thyrosin hydroxylase
T	Section thickness
V	Volume
v/v	Volume per volume
w/v	Weight per volume
ZMNH	Zentrum für Molekulare Neurobiologie Hamburg
%	Percent

µ	micro
µl	microliter
µm	micrometer
°C	Grad Celsius

9 Acknowlegements/Danksagung

Die Arbeit wurde am Institut für Biosynthese neuraler Struktur am Zentrum für molekulare Neurobiologie Hamburg (ZMNH) angefertigt. Ich möchte mich bei Frau Prof. Dr. Melitta Schachner für die Überlassung des interessanten Themas, für die Bereitstellung des Arbeitsplatzes und für die stete Hilfs- und Diskussionsbereitsschaft herzlich bedanken.

Besonders herzlich möchte ich meinem Betreuer Herrn Dr. Andrey Irintchev dafür danken, dass er sowohl während des experimentellen Abschnitts meiner Arbeit als auch während des Schreibens keine Mühen gescheut hat mich in jeglicher Hinsicht zu unterstützten.

Frau Emanuela Szpotowicz danke ich herzlich für die Unterstützung beim Schneiden und Färben der Mausgewebe.

Sehr herzlich danke ich auch Ali Mehanna und Meifang Xiao die mir jederzeit für Fragen aller Art zur Verfügung standen sowie Dag Königrör und Jan Wischweh für die stete Unterstützung bei Fragen zu der technischen Ausarbeitungen des schriftlichen Teils der Arbeit.

Nicht zuletzt danke ich meinen Eltern Frau Juliane Horn und Herrn Ulrich Schmors sowie meinem Lebensgefährten Florian Neumann. Als interessierte, unterstützende, geduldige und verständige Begleiter trugen sie während der gesamten Zeit wesentlich und in vielerlei Hinsicht zum Gelingen dieser Arbeit bei.

10 Eidesstaatliche Versicherung

Ich versichere ausdrücklich, dass ich die Arbeit selbstständig und ohne fremde Hilfe, andere als die von mir angegebenen Quellen und Hilfsmittel nicht benutzt und die aus den benutzen Werken wörtlich oder inhaltlich entnommenen Stellen einzeln nach Ausgaben (Auflage und Jahr des Erscheinens), Band und Seite des benutzen Werkes kenntlich gemacht habe.

Ferner versichere ich, dass ich die Dissertation bisher nicht einem Fachvertreter an einer anderen Hochschule zur Überprüfung vorgelegt oder mich anderweitig um Zulassung zur Promotion beworben habe.

Unterschrift: ……